DMD Fast Forward. Published on October 14, 2008 as doi:10.1124/dmd.108.022178

DMD #22178

Prediction of the Effect of Erythromycin, Diltiazem, and their Metabolites, Alone and in Combination, on CYP3A4 Inhibition

Xin Zhang[1], David R. Jones, and Stephen D. Hall[1]

Division of Clinical Pharmacology, Department of Medicine, Indiana University School of Medicine, Indianapolis, IN (D.R.J. and S.D.H.)

Department of Pharmacy Practice, School of Pharmacy and Pharmaceutical Sciences, Purdue University, Indianapolis, IN (X.Z.)

Running Title: Simultaneous inhibition of CYP3A4

Address Correspondence to: Stephen D. Hall, Ph.D

Eli lilly and Company

Lilly Corporate Center

Drop Code 0720

Indianapolis, IN 46285

Phone: 317-277-0338

Fax: 317-433-9287

E-mail: hallst@lilly.com

Text page : 33

Tables : 4

Figures : 7

References : 34

Abstract : 257 words

Introduction : 456 words

Discussion : 1496 words

Abbreviations used are: DDIs: drug-drug interactions; CYP3A4: cytochrome P450 3A4; ERY: erythromycin; DTZ: diltiazem; nd-ERY: N-desmethylerythromycin; nd-DTZ: N-desmethyldiltiazem; rCYP3A4+b5: cDNA-expressed CYP3A+b5; HLM: human liver microsomes; AUC: area under the plasma concentration-time curve; MIC: metabolic intermediate complex

ABSTRACT

Predictive models of complex drug-drug interactions between multiple inhibitors and their metabolites have not been evaluated. The purpose of this study was to evaluate an interaction model for cytochrome P450 3A4 (CYP3A4) that incorporated the simultaneous reversible and irreversible inhibition by multiple inhibitors. Erythromycin (ERY) and diltiazem (DTZ), and their major metabolites, N-desmethylerythromycin (nd-ERY) and N-desmethyl diltiazem (nd-DTZ), were chosen to evaluate the model. k_{inact} (rate constant for maximal inactivation), K_I (inhibitor concentration at 50% maximal inactivation), and K_i (reversible inhibition constant) were estimated for ERY, DTZ, nd-ERY, and nd-DTZ, respectively, using cDNA-expressed CYP3A4 and human liver microsomes under the optimal experimental conditions. To evaluate the interaction model, combinations of inhibitors and metabolites were incubated at concentrations equal to K_I, ½K_I and 2K_I of each inhibitor for specified durations in both enzyme systems. The models were further evaluated by the incubation of combinations of inhibitors with the substrate testosterone for ten minutes. CYP3A4 inhibition in the presence of drug mixtures was predicted from the inhibition parameters determined for each drug or metabolite alone. The CYP3A4 activity in the presence of multiple inhibitors was well predicted by the model incorporating additive irreversible inhibition as modified by mutual competitive inhibition (% mean error and % mean absolute error ranged from -0.06 to 0.04, and 0.03 to 0.09, respectively). In conclusion, the additive model predicted the combined effect of multiple inhibitors on CYP3A inhibition *in vitro*. However, simultaneous reversible and irreversible inhibition effects should be taken into account in a reaction mixture of substrate and multiple inhibitors of CYP3A4.

INTRODUCTION

Concomitant medications causing drug-drug interactions (DDIs) have led to serious adverse drug events during treatment and resulted in restrictions in prescribing drugs and withdrawal of drugs from the market (Jankel and Fitterman, 1993; Yuan et al., 1999). The incidence and extent of DDIs would be expected to increase when multiple inhibitors of a specific drug-metabolizing enzyme are administered simultaneously compared to a single inhibitor administered alone. According to the FDA's Guidance for Industry Drug Interaction Studies, inhibitors of cytochrome P450 3A4 (CYP3A4) can be classified as potent, moderate, or weak if the area under the plasma concentration-time curve (AUC) fold increase of midazolam with the co-administered inhibitor is more than 5-fold, between 2- and 5-fold, or less than 2-fold, respectively (FDA, 2006). Thus, when two moderate inhibitors, or one moderate and one weak inhibitor are given together, it is likely that they would act as a potent inhibitor. However, to date, studies on DDIs have been exclusively focused on the interactions between two drugs. It is not clear whether the extent of inhibition in the presence of multiple inhibitors is predictable from that of each inhibitor alone since predictive models of complex DDIs involving multiple inhibitors have not been evaluated.

CYP3A4 inhibition can be reversible and/or irreversible. Irreversible inhibition, also referred to as mechanism-based inhibition, is characterized by time-, and inhibitor-concentration-dependent loss of enzyme activity (Silverman, 1988). A mechanism-based inhibitor inhibits the enzyme through irreversibly or quasi-irreversibly binding to the enzyme, thus, the enzyme activity does not return immediately upon elimination of the inhibitor from plasma or tissue (Ito et al., 2003). Interestingly, many clinically significant CYP3A4 inhibitors have been shown to possess, to varying extends, both reversible and irreversible inhibitory effects on CYP3A4 (Zhou et al., 2004). However, whether both effects contribute to the overall extent of inhibition remains unclear.

In a compound mixture where multiple mechanism-based inhibitors are present, their combined effect cannot be assumed to be simply additive due to 1) competition between the inhibitors for the enzyme active site may modulate their inhibition effect; 2) inhibition of the metabolism of each other leads to higher inhibitor concentration compared with each inhibitor alone. The ultimate outcome is determined by the interplay of these factors.

The primary objective of this work is to evaluate a model incorporating competition between the inactivators for the combined effects of multiple irreversible inhibitors. Two representative CYP3A4 inhibitors, the antimicrobial agent erythromycin (ERY) and the calcium channel blocker diltiazem (DTZ), with their major metabolites, N-desmethyl erythromycin (nd-ERY) and N-desmethyl diltiazem (nd-DTZ), were chosen as clinically relevant examples to evaluate the model. DTZ and ERY are moderately strong inhibitors of CYP3A4 *in vivo* causing approximately 4-fold increase in the AUC of oral MDZ (Olkkola et al., 1993; Backman et al.,1994)

MATERIALS AND METHODS

Chemicals and Reagents.

Testosterone (TES), 6β-hydoxytestosterone (6β-OH TES), ERY, DTZ, N-desmethyl diazepam and troleandomycin were purchased from Sigma-Aldrich (St. Louis, MO). nd-ERY was purchased from US Pharmacopeia (Rockville, MD). nd-DTZ was a gift from Tanabe Seiyaku Co. (Osaka, Japan). NADPH (98%) was purchased from Roche Diagnostics (Indianapolis, IN). All other reagents were of high-performance liquid chromatography (HPLC) grade.

cDNA-expressed Human CYP3A4+b5 and Human Liver Microsome.

cDNA-expressed CYP3A4 and cytochrome b5 (rCYP3A4+b5) in insect cell membrane were purchased from BD Gentest (Woburn, MA). One adult human liver microsomal

sample (HLM, IUL-72) was chosen from a liver bank prepared from human liver tissues obtained at surgery in accordance with protocols approved by the Institutional Review Board of Indiana University-Purdue University Indianapolis/Clarian (Indianapolis, IN). Microsomal fractions were prepared as described by Gorski et al and were kept at -80°C (Gorski et al., 1994). The total protein concentration of the HLM was 32 mg/ml (Lowry et al., 1951). The CYP3A4 and CYP3A5 protein concentrations were 25.3 and 0.6 pmol/mg protein, respectively, as quantified by Western blot (Dennison et al, 2007). The CYP3A5 genotype of this human liver was *3/*3 as assessed by real-time reverse transcriptase-polymerase chain reaction as described previously (Dennison et al, 2007).

Quantitation of Reversible Inhibition of CYP3A4 by ERY, nd-ERY, DTZ and nd-DTZ.

To estimate the reversible inhibition constant, K_i, TES and inhibitors were incubated with rCYP3A4+b5 (20 pmol) and HLM (0.1 mg) in sodium phosphate buffer (0.1 M, pH 7.4) and NADPH (1 mM) at 37°C for three minutes. The enzyme reaction was terminated by adding one mL ice-cold acetonitrile. TES concentrations over the range of 10 to 100 μM were used. Concentrations of inhibitors varied over the ranges of 5 to 50 μM (ERY), 5 to 50 μM (nd-ERY), 15 to 120 μM (DTZ), and 0.5 to 20 μM (nd-DTZ) for the incubations with rCYP3A4+b5 and 25 to 200 μM (ERY and nd-ERY), 5 to 160 μM (DTZ), and 0.5 to 20 μM (nd-DTZ) for the incubations with HLM. The three-minute incubation time was chosen to minimize enzyme inactivation during incubation so that the estimated K_i was considered to reflect primarily the binding affinity of the inhibitors to the enzyme.

The reversible inhibition constant K_i was estimated by fitting the appropriate inhibition models (competitive, noncompetitive, or uncompetitive) to the 6β-OH TES formation rate vs. TES concentration data for the incubation for three minutes using nonlinear regression (WinNonlin 4.0; Pharsight, Mountain View, CA). Lineweaver-Burk plots (1/6β-OH TES formation rate vs. 1/TES) were constructed to differentiate modes of inhibition.

Quantitation of Irreversible Inhibition of CYP3A4 by ERY, nd-ERY, DTZ and nd-DTZ.

TES 6β-hydroxylation was used as a marker reaction to quantify CYP3A4 activity. rCYP3A4(+b5) (20 pmol) or HLM (1 mg) were preincubated in a 50 uL reaction mixture with various concentrations of each inhibitor in the presence of NADPH (1 mM) at 37°C for 0, 0.5, 1, and 2 minutes (rCYP3A4+b5) or 0, 1, 2, and 5 min (HLM). Following the preincubation, 950 µL of an incubation mixture containing TES and 1 mM NADPH in 0.1 M sodium phosphate buffer were transferred into the preincubation tube (to achieve a final TES concentration of 200 µM) and further incubated at 37°C for five minutes. The enzyme reaction was terminated by adding 1ml ice-cold acetonitrile. A saturating concentration (10 X K_m) of TES was used to measure the remaining catalytically active CYP3A. The inhibitor concentrations for preincubation with rCYP3A4+b5 ranged from 1 to 50 µM for ERY, 1 to 50 µM for nd-ERY, 0.5 to 15 µM for DTZ and nd-DTZ, respectively. The inhibitor concentrations for preincubation with HLM ranged from 2.5 to 100 µM for ERY and nd-ERY, 2.5 to 20 µM for DTZ, and 0.5 to 15 µM for nd-DTZ, respectively.

To estimate the inactivation parameters, the natural logarithm of the percentage of the remaining CYP3A4 activity was plotted against the preincubation time. The observed pseudo first order rate constants (k_{obs}) were determined from the slopes of the initial linear decline in activity. The parameters k_{inact} and K_I were obtained from simultaneous fitting of the data of the percentage of the remaining activity vs. the preincubation time at all inhibitor concentrations using nonlinear regression (WinNonlin 4.0; Pharsight, Mountain View, CA) according to the following equations:

$$\frac{E_t}{E_0} = e^{-k_{obs} \times t} \quad (1)$$

$$k_{obs} = \frac{k_{inact} \times I}{K_I + I} \quad (2)$$

where E_t and E_0 are enzyme activity at time 0 and t, respectively, k_{obs} is the inactivation rate constant at a given inactivator concentration, k_{inact} is the rate constant that defines the maximal rate of inactive enzyme formation, I is the initial concentration of the inhibitor, and K_I is the inhibitor concentration when $k_{obs} = k_{inact}/2$.

A Model for the Extent of Inactivation in the Presence of Multiple Inhibitors.

This experiment aimed to evaluate the additive characteristic of a model for the prediction of the extent of inactivation by multiple mechanism-based inhibitors. For this purpose, a relative strict condition (ie., inactivation occurs during the initial linear phase, the inhibitor concentration stays constant, and no substrate is present) was applied to avoid confounding factors such as inhibitor depletion or nonlinear decrease of the enzyme activity. Equation X and Y, each generated from Eq. 1, were first evaluated.

$$\text{Equation X} = \frac{E_t}{E_0} = e^{-\sum_{n=1}^{i} k_{obs,n} \times t} = e^{-\sum_{n=1}^{i} \left[\frac{k_{inact,n} \times I_{,n}}{K_{I,n} + I_{,n}} \times t \right]} \quad (3)$$

$$\text{Equation Y} = \frac{E_t}{E_0} = e^{-\sum_{n=1}^{i} k_{obs,n} \times t} = e^{-\sum_{n=1}^{i} \left[\frac{k_{inact,n} \times I_{,n}}{\left[\sum_{m=1}^{j} (1 + \frac{I_{,m}}{K_{i,m}}) \right] \times K_{I,n} + I_{,n}} \times t \right]} \quad (m \neq n) \quad (4)$$

In Equation X and Y, n refers to the number of different inhibitors (1 to i) in the reaction mixture. In Equation Y, m represents all the inhibitors other than the i^{th} inhibitor, ie., m≠n. In Equation X, the inactivation rate constant, k_{obs}, of each inhibitor was added to account for their combined effects. In Equation Y, K_I of each inhibitor was further modified by

DMD Fast Forward. Published on October 14, 2008 as DOI: 10.1124/dmd.108.022178
This article has not been copyedited and formatted. The final version may differ from this version.

$\left[\sum_{m=1}^{j}(1+\frac{I,_m}{K_{i,m}})\right]$, where $I,_m$ and $K_{i,m}$ are the concentration and competitive inhibition constant of the coexisting inhibitors, respectively, assuming the inhibitors will compete with each other for the enzyme active site. The percentage of remaining enzyme activity in Equation X and Y was calculated from the estimated inhibition parameters (k_{inact}, K_I, and K_i) for each inhibitor alone, inhibitor concentrations, and the preincubation times.

To test Equation X and Y, inhibitors were incubated in combination (ERY + DTZ, ERY + nd-ERY, DTZ + nd-DTZ, and all four compounds together) at concentrations equal to ½K_I, K_I, and 2K_I of each inhibitor for one and two minutes with rCYP3A4 +b5; and two and five minutes with HLM. The percentage of remaining enzyme activity was measured as described above. The brief incubation time was used because Equation X and Y follow the same assumption as Eq. 1, ie., the reactions under the initial linear range and the inhibitor depletion was minimal. The predicted and observed percentages of remaining enzyme activity were compared for Equation X and Y.

Time Course of CYP3A Inactivation

To quantify the percentage of remaining CYP3A activity, and the inhibitor and metabolite concentrations with time, rCYP3A4+b5 (20 pmol) and HLM (1 mg) were incubated with ERY, nd-ERY, DTZ, and nd-DTZ, alone and in combination, for a period of ten minutes. For each time point, two identical tubes were prepared. At 0, 0.5, 1, 2, 5, and 10 minutes after the initiation of the reaction, 950 µL of incubation mixture containing TES (to achieve a final TES concentration of 200 µM) and 1 mM NADPH in 0.1 M sodium phosphate buffer were transferred into one tube to estimate the remaining enzyme activity. The other tube was quenched with one mL ice cold acetonitrile for the measurement of the inhibitor and metabolite concentrations at the specified time points. Vehicle controls (ie., no inhibitors) were run to account for any decrease in enzyme activity with time under these conditions. Experiments were performed in duplicate.

DMD Fast Forward. Published on October 14, 2008 as DOI: 10.1124/dmd.108.022178
This article has not been copyedited and formatted. The final version may differ from this version.

Predictive Models for a compound mixture containing the substrate and multiple inhibitors

A more general situation for DDIs (both *in vitro* and *in vivo*) is that the substrate coexists with the inhibitor in a reaction mixture, and the inhibitor and substrate may coexist for a period of time that is longer than the initial linear phase of enzyme inactivation. Therefore, Equation X and Y were further tested in an incubation for ten minutes, which is out of the initial linear phase, and in the presence of the substrate, TES. TES and inhibitor concentrations used for the ten-minute incubation with a single inhibitor were the same as those used for the three-minute incubation. For the incubations of TES with multiple inhibitors, a concentration at its K_m in each enzyme system was used. The formation rate of 6β-OH TES was measured as described earlier.

The following three candidate models incorporating reversible (Model A) or irreversible (Model B) inhibition, or both (Model C), were evaluated for the prediction of inhibition of CYP3A4 activity by single or multiple inhibitors.

Model A $$R_{6b\text{-}OH\ TES} = \frac{V_{max} \times S}{K_m \times (1 + \frac{I_{,1}}{K_{i,1}} + ... + \frac{I_{,n}}{K_{i,n}}) + S} \quad (5)$$

Model B $$R_{6b\text{-}OH\ TES} = \frac{V_{max} \times (a \times Y + b \times e^{-c \times t}) \times S}{K_m + S} \quad (6)$$

Model C $$R_{6b\text{-}OH\ TES} = \frac{V_{max} \times (a \times Y + b \times e^{-c \times t}) \times S}{K_m \times (1 + \frac{\bar{I}_{,1}}{K_{i,1}} + ... + \frac{\bar{I}_{,n}}{K_{i,n}}) + S} \quad (7)$$

In the above models, V_{max}, K_m, and S are the maximal rate and the Michaelis-Menten constant for 6β-OH TES formation, and TES concentration, respectively. In Model A, I is

the nominal inhibitor concentration, assuming no inhibitor depletion during competitive inhibition. In Model B and C, a time-averaged inactivator concentration ($\bar{I}$) was used to represent the true inhibitor concentration in the mixture due to possible inhibitor depletion during a ten-minute incubation. $\bar{I}$ was calculated by Eq. 8 where AUC_{0-10} is the area under the inhibitor concentration–time curve from zero to 10 minutes estimated with noncompartment analysis using the trapezoidal rule in WINONLIN (Version 3.01; Pharsight, Mountain View, CA). The time averaged inhibitor concentration was calculated by dividing this AUC by 10 minutes.

$$\bar{I} = \frac{AUC_{0-10}}{10} \quad (8)$$

In Model B and C, only Equation Y was incorporated for the loss of enzyme of activity due to mechanism-based inhibition by single or multiple inhibitors because preliminary studies suggested Equation Y better predicted the remaining enzyme activity than Equation X. Furthermore, because preliminary study showed bi-exponential decrease of enzyme activity during the incubation of ten minutes and Equation Y can account only for the initial linear phase, a second term was incorporated as shown in Eq. 9, where a, b, and c were estimated by curve-stripping of the plot of the percentage of remaining enzyme activity against time.

$$\frac{E_t}{E_0} = a \times e^{-k_{obs} \times t} + b \times e^{-c \times t} \quad (9)$$

In Model A, B, and C, V_{max} and K_m of TES were estimated by incubating TES at various concentrations with rCYP3A4 +b5 and HLM for five minutes and fitting the 6□-OH TES formation rate vs. TES concentration data to Michaelis-Menten equation. When there was substrate present, S/K_m was also included in the term that modified the K_I of each

DMD Fast Forward. Published on October 14, 2008 as DOI: 10.1124/dmd.108.022178
This article has not been copyedited and formatted. The final version may differ from this version.

inhibitor. S was TES concentration. The value of K_m estimated was used as the K_i for TES.

Quantitation of 6β-OH TES, ERY, nd-ERY, DTZ, and nd-DTZ by HPLC and LC/MS.

6β-OH TES concentration was determined by an HPLC system with ultraviolet detection at a wavelength of 254 nm as previously described (Zhao et al., 2002).

For the determination of ERY and nd-ERY concentrations, 200 µL of internal standard (TAO, 0.5ng/ul in 1 M sodium cabonate/1 M sodium bicarbonate, v/v = 4:1, pH = 9.6) was added to each sample, followed by the addition of 3 mL Hexane/ethylacetate (v:v, 1:1). Chromatographic separation of the analytes and internal standard was accomplished with a Phenomenex Luna C18 column (3 µM × 2 mm i.d. × 150 mm). The mobile phase consisted of a mixture of acetonitrile:methanol:Ammonium Acetate (0.25 M, pH=7.6) (200:75:225 v/v/v), and was pumped at a flow rate of 0.2 mL/min. The effluent was delivered to a mass spectrometer (Navigator™, Finnigan, San Jose, CA) interfaced with a Hewlett Packard 1100 binary pump equipped with a HP1100 autosampler. The ESI probe was run in the positive ion mode with probe temperatures of 300 °C. ERY, nd-ERY and troleandomycin were detected in the selected ion recording mode at m/z 734, 720, and 771, respectively.

The concentrations of DTZ and nd-DTZ were determined based on a previous method with modification (Gorski et al., 1999). Briefly, the reaction mixture was extracted with eight mL ethylacetate after the addition of 0.5 mL of 0.5 M sodium hydroxide/glycine buffer (pH=8.5) Chromatographic separation of the analytes and internal standard was accomplished with a Phenomenex Luna C18 column (5 µM × 4.6 mm i.d. × 150 mm). The mobile phase consisted of a mixture of methanol/100 mM ammonium acetate (75:25 v/v) and was pumped at a flow rate of 1 mL/min. The effluent was delivered to a mass spectrometer (Navigator™, Finnigan, San Jose, CA) interfaced with a Hewlett Packard 1100 binary pump equipped with a HP1100 autosampler. The ESI probe was run in the

positive ion mode with probe temperatures of 400 °C. DTZ, nd-DTZ, and N-desmethyldiazepam were detected in the selected ion recording mode at m/z 414, 401, and 271, respectively.

Data Analysis.

Percent mean error (%ME) and percent mean absolute error (%MAE) were calculated as following and served as measures of bias and precision, respectively, for the predictions:

$$\%\text{ME} = \frac{\frac{1}{n}\sum(\text{predicted value} - \text{observed value})}{\text{predicted value}} \quad (10)$$

$$\%\text{MAE} = \frac{\frac{1}{n}\sum|\text{predicted value} - \text{observed value}|}{\text{predicted value}} \quad (11)$$

where n is the number of predictions.

A 2-tailed Student t test was performed to compare the %ME and %MAE calculated for different models. Differences were considered statistically significant at $P < .05$.

RESULTS

Reversible and Irreversible Inhibition of CYP3A4 by ERY, nd-ERY, DTZ, and nd-DTZ.

All four compounds (ERY, DTZ, nd-ERY, and nd-DTZ) displayed time- and concentration-dependant inhibition of CYP3A4 with rCYP3A4+b5 and HLM, with the major metabolite of ERY, nd-ERY, being characterized as a mechanism-based inhibitor for the first time (Fig. 1). Fig. 2 shows the plots of k_{obs} against inhibitor concentrations for all four compounds with rCYP3A4+b5 and HLM. The estimated k_{inact} and K_I for CYP3A4 were obtained by fitting the inactivation profiles to Eq. 1, and are summarized in Table 1. The values of K_I and k_{inact} estimated with rCYP3A4+b5 were approximately 3-fold lower and 4-fold higher than those estimated with HLM, respectively, for all four compounds. Based on the ratio of k_{inact}/K_I, the inactivation efficiency of nd-ERY is comparable with that of ERY (k_{inact}/K_I for nd-ERY and ERY are 60 and 70 $min^{-1}nM^{-1}$ in rCYP3A4+b5, and 9 and 6 $min^{-1}nM^{-1}$ in HLM, respectively); whereas nd-DTZ appears to be more potent than DTZ (k_{inact}/K_I = 1333 and 220 $min^{-1}nM^{-1}$ for nd-DTZ and DTZ with rCYP3A4+b5, and 133 and 20 $min^{-1}nM^{-1}$with HLM, respectively).

To evaluate reversible inhibition, each compound was incubated with TES in rCYP3A4+b5 and HLM for three minutes. The three-minute incubation time was chosen to minimize enzyme inactivation during incubation so that the estimated K_i was considered to reflect primarily the binding affinity of the inhibitors to the enzyme. All four compounds displayed competitive inhibition of CYP3A4 (data not shown). ERY and nd-ERY have comparable values of K_i (Table 2). DTZ appears to be a more efficient competitive inhibitor of CYP3A4 with rCYP3A4+b5 (K_i = 5.9 μM) than with HLM (K_i = 41 μM), and nd-DTZ is a potent competitive inhibitor of CYP3A4 with both systems with K_i approaching K_I (Table 2).

DMD Fast Forward. Published on October 14, 2008 as DOI: 10.1124/dmd.108.022178
This article has not been copyedited and formatted. The final version may differ from this version.

The effect of incubation time on K_i estimation was evaluated. Compared with the K_i estimated with the three-minute incubation, the K_i estimated with the ten-minute incubation are generally smaller, as illustrated in Table 2. Fig. 3 shows the Lineweaver-Burk plot for three- and ten-minute incubation of TES and nd-DTZ with rCYP3A4+b5. The fitted lines for different inhibitor concentrations converged on the y-axis for the three-minute incubation, suggesting competitive inhibition. In contrast, for the ten-minute incubation, the intercept on y-axis, which represents $1/V_{max}$, is higher for higher nd-DTZ concentration. This is probably due to more significant time-dependant inactivation by nd-DTZ occurring during ten-min incubation than three-minute incubation.

A Model for the Extent of Inactivation in the Presence of Multiple Inhibitors

Equation X and Y were first evaluated in an incubation of the inhibitors (in the absence of substrate) with CYP3A4 for a brief incubation time that ensured inactivation occurred within the initial linear phase. The predicted percentage of remaining enzyme activity calculated using Equation X and Y was plotted against the observed percentage of remaining enzyme activity obtained from experiments for the combination of ERY+DTZ, ERY+nd-ERY, DTZ+nd-DTZ, and all four compounds together with rCYP3A4+b5 and HLM. Fig. 4 shows the plots for ERY+DTZ (A) and DTZ+ nd-DTZ (B) with HLM. Overall, good correlation was observed for both combinations using Equation X and Y, with Equation Y having a better predictive performance. For example, for ERY+DTZ with HLM, the %ME, an indicator of the closeness of the predicted values to the observed values, was significantly lower using Equation Y compared to Equation X (0.008 ± 0.06 vs. -0.08 ± 0.06, $p<0.05$, Table 3); for DTZ+nd-DTZ, the %ME was -0.02 ± 0.06 and -0.08 ± 0.08 using Equation X and Y, respectively, $p<0.05$, Table 3). The %ME was significantly lower using Equation Y than Equation X ($p<0.05$) for all the other predictions, as listed in Table 3. The %MAE, an indicator of the precision of the prediction, was similar in most cases for using both equations, indicating comparable precision.

Changes of the Percentage of Remaining Enzyme Activity, Parent Drug and Metabolite Concentrations with Time

Fig. 5A shows the time profiles for percentage of remaining enzyme activity, inhibitor and metabolite concentrations, and enzyme degradation after incubation of ERY at 2.5, 5, and 10 μM (ie., at $1/2K_I$, K_I, and $2K_I$) with rCYP3A4+b5 for ten minutes. The ten-minute incubation reveals a bi-exponential decrease of percentage of remaining enzyme activity at all three ERY concentrations. There was an initial rapid decline within the first two minutes followed by a slower decrease phase up to ten minutes. A similar pattern was observed for the ten-minute incubation of other compounds in both systems. Also, the ERY concentration-time profile showed significant depletion of ERY with rCYP3A4+b5 at later time points with ERY concentrations falling from 2.5, 5, and 10 μM to 0.17, 0.74, and 3.4 μM, respectively. Furthermore, the decline of ERY concentration was approximately in parallel with the decline of enzyme activity. An early rapid depletion of ERY was accompanied by the appearance of nd-ERY. At the lower ERY concentrations, the concentrations of nd-ERY appeared to reach a plateau for all three ERY concentrations tested. The time profiles of percentage of remaining enzyme activity and inhibitor concentrations after the incubation of multiple inhibitors were also investigated. As shown in Fig. 5B, when 5 μM ERY and 1 μM DTZ (ie., at their respective K_I in rCYP3A4+b5) were incubated together, there was a further decrease in the percentage of remaining enzyme activity, compared to each inhibitor alone, at all time points. Using Eq. 8, time-averaged ERY concentration in the absence and presence of DTZ were 1.7 and 2 μM, respectively; and time-averaged DTZ concentration increased from 0.2 to 0.27 μM when there was ERY present in the incubation. These increases in the inhibitor concentrations resulted in insignificant changes in the % remaining enzyme activity using Equation X and Y or Model A, B, and C (data not shown).

DMD Fast Forward. Published on October 14, 2008 as DOI: 10.1124/dmd.108.022178
This article has not been copyedited and formatted. The final version may differ from this version.

Prediction of the Interactions between TES and Multiple Inhibitors Considering Reversible and Irreversible Inhibition

To further test the additive model in the context of a compound mixture containing inhibitors and substrate incubated for a longer period of time (ten minutes), inhibitors (alone and in combination) and TES were incubated with rCYP3A4+b5 and HLM for ten minutes. The V_{max} and K_m (mean ± SD) estimated for 6β-OH TES formation were 2650 ± 10.9 pmol/min and 28 ±1 μM with rCYP3A4+b5 and 286 ± 8.4 pmol/min and 58.6 ± 1.2 μM with HLM, respectively. Fig. 6 shows the representative plots of the predicted vs. observed 6β-OH TES formation rate for the incubation of TES with ERY (Fig. 6A) and TES with nd-DTZ (Fig. 6B) for ten minutes with rCYP3A4+b5 using Model A, B, and C. For ERY, Model A (competitive inhibition model) overestimated the 6β-OH TES formation rate (ie., underestimated the extent of inhibition by ERY) whereas the predicted and observed 6β-OH TES formation rate were in good agreement using either Model B or C (%ME was 0.93, 0.06, and -0.01 for Model A, B, and C, respectively). In contrast, both Model A and B underestimated the inhibition of 6β-OH TES formation by nd-DTZ, whereas the observed 6β-OH TES formation rate was excellently predicted by Model C, suggesting both reversible and irreversible inhibition need to be considered, especially for compounds that also exhibit strong reversible inhibition. The %ME (mean ± SD) was significantly higher for Model A than Model C, or for Model B than Model C (1.00 ± 0.38, 0.26 ± 0.21, and -0.07 ± 0.19 for Model A, B, and C, respectively). The %ME and %MAE values calculated for the three models for all the predictions are listed in Table 4. Overall, the 6β-OH TES formation rate was best predicted by Model C for all compounds (%ME for Model C was the lowest, and was significantly lower than that for Model A for all the predictions as indicated by the *p* values). Model B significantly overestimated the 6β-OH TES formation rate for all the incubations tested except for ERY and nd-ERY with both enzyme systems.

Fig. 7 shows the representative plots of the predicted against observed 6β-OH TES formation rate for the incubation of TES and the combination of ERY+DTZ (Fig.7A), and TES and ERY+DTZ+nd-ERY+nd-DTZ (Fig.7B) with HLM. The predicted vs. observed 6β-OH TES formation rate agreed the best with each other using Model C for both combinations. As also shown in Table 4, the %ME was significantly lower for Model C than Model A or B for the prediction of all the combinations, indicating the best predictive performance of Model C among the three models.

DISCUSSION

DDIs remain a serious problem in clinical practice and the development of new drugs (Lazarou et al., 1998; Gandhi et al., 2003). Predictive models for complex DDIs involving multiple inhibitors and their metabolites are not readily available, making it infeasible to predict *in vivo* DDIs involving multiple inhibitors from *in vitro* data. The current study for the first time evaluated an interaction model for the combined effect of multiple inhibitors on CYP3A4 inhibition *in vitro*. The combined effect of multiple inhibitors can be well predicted by the additive model (Equation Y) where the inactivation rate constant of each inhibitor were added and the competition between coexisting inhibitors was considered. The results in this study also suggest that simultaneous reversible and irreversible inhibition effects need to be taken into account (Model C) in a compound mixture involving multiple inhibitors and their metabolites. Furthermore, characterization of the bi-exponential decline of remaining enzyme activity in an incubation with a mechanism-based inhibitor was shown to be important for the prediction, although the mechanism under this phenomenon remains unclear.

Due to the dual effect of a mechanism-based inhibitor as a competitive inhibitor and an inactivator of the enzyme, reversible and irreversible inhibition parameters were first estimated separately for all the four compounds under optimal experimental conditions (ie., the measurement of the inactivation effect was not obscured by the competitive inhibition effect, and *vice versa*). The widely adopted approach for mechanism-based inhibition consists of a “pre-incubation” stage followed by an “incubation” stage (Silverman, 1988). However, efforts have not always been exerted to meet the two important assumptions that there is negligible metabolism of the inhibitor during the “pre-incubation” stage, and that negligible enzyme inactivation occurs during the “incubation” stage to ensure the accuracy in parameter estimation (Yang et al., 2005).

A considerable range of preincubation time and dilution factors have been used across laboratories, leading to great discrepancies in the estimates of the inactivation parameters (Ghanbari et al., 2006). Our study was designed to minimize the preincubation and incubation times, and maximize the dilution factor. Specifically, a brief preincubation time (two-minute for rCYP3A4+b5 and five-minute for HLM), a relatively high dilution factor (20-fold) and a short incubation time (five-minute) were applied in this study. Similarly, for the estimation of the competitive inhibition constant, K_i, the incubation time was kept brief (three-minute) so that the estimated K_is were considered to reflect primarily the initial binding of the inhibitor to the enzyme with minimal inactivation occurring. The differences in the K_i values estimated using data from the three- and ten-minute incubations (Table 2 and Fig. 3) further confirmed the impact of incubation time on the estimation of this parameter. Moreover, the Lineweaver-Burk plot suggested competitive inhibition of 6β-OH TES formation by nd-DTZ in the three-minute incubation, indicating no significant inactivation occurred during the three-minute incubation. Thus the estimation of K_i using three-minute incubation was considered appropriate. In contrast, the intercepts on y-axis were higher for higher nd-DTZ concentrations with the ten-minute incubation, suggesting lower V_{max} at higher inhibitor concentration, probably due to enzyme inactivation occurring with time. Caution should be exerted with differentiating inhibition patterns using Lineweaver-Burk plot alone, because the plot for the ten-minute incubation could be misinterpreted as non-competitive or uncompetitive inhibition (Fig. 3).

A simple rearrangement of Equation X shown in Eq. 12 suggests that Equation X actually reflects that the % remaining enzyme activity in the presence of two inhibitors can be predicted by the product of the % remaining activity of each inhibitor alone.

DMD Fast Forward. Published on October 14, 2008 as DOI: 10.1124/dmd.108.022178
This article has not been copyedited and formatted. The final version may differ from this version.

$$\%\frac{E_t}{E_0}(A+B) = e^{-(k_{obs,A}+k_{obs,B})\times t} = e^{-k_{obs,A}\times t}\times e^{-k_{obs,B}\times t} = \%\frac{E_t}{E_0}(A)\times\%\frac{E_t}{E_0}(B) \quad (12)$$

Nevertheless, it is not surprising that Equation X overestimated the extent of inhibition for all the combinations tested in both rCYP3A4 and HLM (Fig. 4 and Table 3). A major reason for this discrepancy is most likely due to competition between inhibitors that is not considered. After the K_I of each inhibitor was modified by $(1+\sum I/K_i)$ of all the coexisting inhibitors, the prediction performance was significantly improved for all the combinations tested. On the other hand, in a reaction mixture of two inhibitors, one would expect that mutual inhibition of the metabolism of each other may lead to an increase in the concentrations of each inhibitor, which in turn, may enhance the inhibition effect compared to that of each inhibitor alone. However, as shown in Fig. 5, when ERY and DTZ were incubated together at their K_I, the concentrations of ERY (or DTZ) in the presence and absence of DTZ (or ERY) are comparable. This was also observed at other concentrations of inhibitors tested (1/2 K_I and 2 K_I). To this end, Equation Y was proven to be an appropriate model for the combined effect of multiple inhibitors.

Equation Y was further evaluated under conditions where the substrate and inhibitor(s) were added simultaneously to the reaction mixture and incubated for ten minutes (exceeding the initial linear phase). For this purpose, the change of percentage of remaining enzyme activity, inhibitor and metabolite concentration with time during a ten-minute incubation was examined. Fig. 5 indicates a bi-exponential decline of percentage of remaining enzyme activity throughout the ten-minute incubation. Since the commonly-used equation for mechanism-based inhibition (Eq. 1) is only valid for the initial linearly declining phase, there would be significant overestimation for the extent of inhibition if applying Eq. 1 for the whole ten-minute incubation. However, the factors that might cause the subsequent slower phase are not clear yet. Preliminary data in our lab

suggests it is not likely to be due to the decrease in inhibitor concentrations (data not shown). Therefore, a descriptive model was applied for the second phase as shown in Eq. 9, where a, b, and c were constants estimated by curve-stripping of the percentage of remaining enzyme activity vs. time plot. The significant depletion of the inhibitor at later time points is consistent with other observations, and is probably due to the inhibitor being either complexed with the enzyme through MIC formation or converted to the metabolite (Zhao et al., 2005; McGinnity et al., 2006). However, there was a failure to achieve mass-balance with an accounting of the measured metabolite (nd-ERY) and the loss of enzyme activity due to the irreversible ERY binding, suggesting that other metabolites formed (data not shown).

Furthermore, the relative contribution of reversible and irreversible inhibition was studied for the incubation of a mechanism-based inhibitor with the substrate. Fig. 6 showed the predicted vs observed 6β-OH TES formation rate when ERY (Fig. 6A or nd-DTZ (Fig. 6B) was incubated with TES. For a drug like ERY, which acts as an effective mechanism-based inhibitor but weak reversible inhibitor, competitive inhibition model (Model A) significantly underestimated while inactivation model (Model B) was generally close to the model that incorporates simultaneous reversible and irreversible inhibition (Model C) at concentrations tested (1/2 K_I, K_I, and $2K_I$), indicating inactivation is what mainly occurred in the reaction mixture. In contrast, for nd-DTZ, which represents the group of compounds which are effective as both reversible and irreversible inhibitors, both model A and model B underestimated the inhibition extent. Therefore, as a whole, Model C was considered as the best model for a mechanism-based inhibitor which exhibits either high or low potency as a reversible inhibitor. On the other hand, Model C incorporating Equation Y best estimated 6□-OH TES formation rate in a mixture where TES was incubated with multiple inhibitors simultaneously, further suggesting the validity of the interaction model (Equation Y).

Prediction of the magnitude of *in vivo* DDIs using *in vitro* inhibition data has been a routine strategy applied to reduce the number of *in vivo* studies required and guide the design of clinical trials (Ito et al., 1998). It has been successful for single inhibitor interaction for many cases (Obach et al., 2006; Obach et al., 2007). With the validation of the additive model in this study, prediction of the extent of inhibition with multiple inhibitors has been made possible. This is of particular importance since clinical studies for all possible combinations of inhibitors are not feasible.

Consistent with previous findings, the K_I and K_i estimated with rCYP3A4+b5 were generally lower and k_{inact} is higher than that estimated with HLM (Table 1 and 2) in this study (McConn et al., 2004). A possible explanation is higher non-specific protein binding and different lipid environment in HLM compared to recombinant enzyme system. Interestingly, McGinnity and colleagues reported that the inhibition parameters (k_{inact} and K_I) estimated in cultured primary human hepatocytes generally were in good agreement with the values derived using HLMs (McGinnity et al., 2006). Thus, caution should be exercised when making prediction of the extent of *in vivo* DDIs using parameters estimated from recombinant enzyme.

To summarize, nd-ERY and ERY have comparable inhibition potency while nd-DTZ is more potent than DTZ as a CYP3A4 inhibitor. The additive model incorporating competition between inhibitors (Equation Y) is appropriate for the prediction of the extent of inhibition in the presence of multiple inhibitors. Moreover, simultaneous reversible and irreversible inhibition effects should be taken into account in a reaction mixture of multiple inhibitors and substrate of CYP3A4.

ACKNOWLEGEMENT

The authors would like to acknowledge the contributions of Mitch Hamman and Narjis Zaheer to this manuscript.

REFERENCES

Backman JT, Olkkola KT, Aranko K, Himberg JJ and Neuvonen PJ (1994) Dose of midazolam should be reduced during diltiazem and verapamil treatments. Br J Clin Pharmacol **37**:221-5.

Bensoussan C, Delaforge M and Mansuy D (1995) Particular ability of cytochromes P450 3A to form inhibitory P450-iron-metabolite complexes upon metabolic oxidation of aminodrugs. Biochem Pharmacol **49**:591-602.

Dennison JB, Jones DR, Renbarger JL and Hall SD (2007) Effect of CYP3A5 expression on vincristine metabolism with human liver microsomes. J Pharmacol Exp Ther **321**:553-563.

[FDA] Food and Drug Administration, U.S. Department of Health and Human Services: Guidance for Industry: In Vivo Drug Metabolism/Drug Interaction Studies: Study Design, Data Analysis, and Recommendations for Dosing and Labeling. September 2006 [Online]. Available: http://www.fda.gov/cder November 2006.

Gandhi TK, Weingart SN, Borus J, Seger AC, Peterson J, Burdick E, Seger DL, Shu K, Federico F, Leape LL and Bates DW (2003) Adverse drug events in ambulatory care. N Engl J Med **348**:1556-1564.

Ghanbari F, Rowland-Yeo K, Bloomer JC, Clarke SE, Lennard MS, Tucker GT and Rostami-Hodjegan A (2006) A critical evaluation of the experimental design of studies of mechanism based enzyme inhibition, with implications for in vitro-in vivo extrapolation. Curr Drug Metab **7**:315-334.

Gorski JC, Hall SD, Jones DR, VandenBranden M and Wrighton SA (1994) Regioselective biotransformation of midazolam by members of the human cytochrome P450 3A (CYP3A) subfamily. Biochem Pharmacol **47**:1643-1653.

Ito K, Iwatsubo T, Kanamitsu S, Ueda K, Suzuki H and Sugiyama Y (1998) Prediction of pharmacokinetic alterations caused by drug-drug interactions: metabolic interaction in the liver. Pharmacol Rev **50**:387-412.

Ito K, Ogihara K, Kanamitsu S and Itoh T (2003) Prediction of the in vivo interaction between midazolam and macrolides based on in vitro studies using human liver microsomes. Drug Metab Dispos **31**:945-954.

Jankel CA and Fitterman LK (1993) Epidemiology of drug-drug interactions as a cause of hospital admissions. Drug Saf 9:51-59.

Jones DR and Hall SD (2002) Mechanism-based inhibition of human cytochromes P450: in vitro kinetics and in vitro-in vivo correlations. In Drug-drug Interactions, Marcel Dekker, New York.

Jones DR, Gorski JC, Hamman MA, Mayhew BS, Rider S and Hall SD (1999) Diltiazem inhibition of cytochrome P-450 3A activity is due to metabolite intermediate complex formation. J Pharmacol Exp Ther **290**:1116-1125.

Lampen A, Christians U, Guengerich FP, Watkins PB, Kolars JC, Bader A, Gonschior AK, Dralle H, Hackbarth I and Sewing KF (1995) Metabolism of the immunosuppressant tacrolimus in the small intestine: cytochrome P450, drug interactions, and interindividual variability. Drug Metab Dispos **23**:1315-1324.

Lazarou J, Pomeranz B and Corey P (1998) Incidence of adverse drug reactions in hospitalized patients: a meta-analysis of prospective studies. JAMA **279**:200-1205.

Lowry OH, Rosebrough NJ, Farr AL and Randall RJ (1951) Protein measurement with the Folin phenol reagent. J Biol Chem **193**:265-275.

Marre F, de Sousa G, Orloff AM and Rahmani R (1993) In vitro interaction between cyclosporin A and macrolide antibiotics. Br J Clin Pharmacol **35**:447-448.

Mayhew BS, Jones DR and Hall SD (2000) An in vitro model for predicting in vivo inhibition of cytochrome P450 3A4 by metabolic intermediate complex formation. Drug Metab Dispos **28**:1031-1037.

McConn DJ, 2nd, Lin YS, Allen K, Kunze KL and Thummel KE (2004) Differences in the inhibition of cytochromes P450 3A4 and 3A5 by metabolite-inhibitor complex-forming drugs. Drug Metab Dispos **32**:1083-1091.

McGinnity DF, Berry AJ, Kenny JR, Grime K and Riley RJ (2006) Evaluation of time-dependent cytochrome P450 inhibition using cultured human hepatocytes. Drug Metab Dispos **34**:1291-1300.

Murray M and Butler AM (1996) Enhanced inhibition of microsomal cytochrome P450 3A2 in rat liver during diltiazem biotransformation. J Pharmacol Exp Ther **279**:1447-1452.

Obach RS, Walsky RL and Venkatakrishnan K (2007) Mechanism-based inactivation of human cytochrome p450 enzymes and the prediction of drug-drug interactions. Drug Metab Dispos **35**:246-255.

Obach RS, Walsky RL, Venkatakrishnan K, Gaman EA, Houston JB and Tremaine LM (2006) The utility of in vitro cytochrome P450 inhibition data in the prediction of drug-drug interactions. J Pharmacol Exp Ther **316**:336-348.

Ohmori S, Ishii I, Kuriya S, Taniguchi T, Rikihisa T, Hirose S, Kanakubo Y and Kitada M (1993) Effects of clarithromycin and its metabolites on the mixed function oxidase system in hepatic microsomes of rats. Drug Metab Dispos **21**:358-363.

Olkkola KT, Aranko K, Luurila H, Hiller A, Saarnivaara L, Himberg JJ and Neuvonen PJ (1993) A potentially hazardous interaction between erythromycin and midazolam. Clin Pharmacol Ther. **53**:298-305.

Omura T and Sato R (1964) The Carbon Monoxide-Binding Pigment Of Liver Microsomes. I. Evidence For Its Hemoprotein Nature. *J Biol Chem* **239:**2370-2378.

Pichard L, Fabre I, Fabre G, Domergue J, Saint Aubert B, Mourad G and Maurel P (1990) Cyclosporin A drug interactions. Screening for inducers and inhibitors of cytochrome P-450 (cyclosporin A oxidase) in primary cultures of human hepatocytes and in liver microsomes. *Drug Metab Dispos* **18:**595-606.

Silverman R (1988) *Mechanism-based enzyme inactivation: chemintry and enzymology*. CRC Press, Boca Raton (FL).

Sugihara J, Sugawara Y, Ando H, Harigaya S, Etoh A and Kohno K (1984) Studies on the metabolism of diltiazem in man. *J Pharmacobiodyn* **7:**24-32.

Wang YH, Jones DR and Hall SD (2004) Prediction of cytochrome P450 3A inhibition by verapamil enantiomers and their metabolites. *Drug Metab Dispos* **32:**259-266.

Yang J, Jamei M, Yeo KR, Tucker GT and Rostami-Hodjegan A (2005) Kinetic values for mechanism-based enzyme inhibition: assessing the bias introduced by the conventional experimental protocol. *Eur J Pharm Sci* **26:**334-340.

Yeung PK, Buckley SJ, Hung OR, Pollak PT, Barclay KD, Feng JD, Farmer PS and Klassen GA (1996) Steady-state plasma concentrations of diltiazem and its metabolites in patients and healthy volunteers. *Ther Drug Monit* **18:**40-45.

Yuan R, Parmelee T, Balian JD, Uppoor RS, Ajayi F, Burnett A, Lesko LJ and Marroum P (1999) In vitro metabolic interaction studies: experience of the Food and Drug Administration. *Clin Pharmacol Ther* **66:**9-15.

Zhao P, Kunze KL and Lee CA (2005) Evaluation of time-dependent inactivation of CYP3A in cryopreserved human hepatocytes. *Drug Metab Dispos* **33:**853-861.

Zhao XJ, Jones DR, Wang YH, Grimm SW and Hall SD (2002) Reversible and irreversible inhibition of CYP3A enzymes by tamoxifen and metabolites. *Xenobiotica* **32:**863-878.

Zhou S, Chan E, Lim LY, Boelsterli UA, Li SC, Wang J, Zhang Q, Huang M and Xu A (2004) Therapeutic drugs that behave as mechanism-based inhibitors of cytochrome P450 3A4. *Curr Drug Metab* **5:**415-442.

FOOTNOTES

[1]Current affiliation: Department of Drug Disposition, Eli Lilly and Company, Lilly Corporate Center, Indianapolis, Indiana 46285.

FIGURE LENGENDS

Fig. 1. Plot of percentage of remaining CYP3A4 activity against preincubation time for nd-ERY incubation with HLM.

nd-ERY at 2.5 μM (●), 10 μM (■), 25 μM (▲), and 100 μM (♦) was incubated with HLM (1 mg) in a 50 μL reaction mixture in the presence of NADPH (1 mM) at 37°C for 0, 1, 2, and 5 minutes. The remaining enzyme activity was quantified by adding 950 μL of incubation mixture containing 200 μM TES and further incubating at 37°C for five minutes. Individual data points represent the mean result from duplicate incubations. Error bars are SD. The lines represent the simultaneous fit of data at all inhibitor concentrations.

Fig. 2. Plots of k_{obs} against inhibitor concentration of ERY(●) and nd-ERY(○) in rCYP3A4(+b5) (A) and HLM (B); and DTZ(●) and nd-DTZ(○) in rCYP3A4(+b5) (C) and HLM (D).

k_{obs} value estimated from the slope of the initial linear decline phase of the % remaining CYP3A4 activity against preincubation time plot for each inhibitor concentration was plotted against inhibitor concentration. Each point represents the mean of duplicate samples. The solid and broken line represents the predicted k_{obs} values using the estimates of the parameters from the simultaneous fits (Eq.1) for parent drugs and metabolites, respectively.

Fig. 3. Lineweaver-Burk plot for the inhibition of CYP3A4 by nd-DTZ in an incubation for three (A) and ten (B) minutes.

TES (10 ~ 100 μM) and nd-DTZ at 0, 0.5, 2, and 6 μM were incubated with rCYP3A4(+b5) (20 pmol) at 37°C for three and ten minutes. The lines are best fit of data at each inhibitor concentration.

Fig. 4. Plot of predicted against observed %remaining enzyme activity for the incubation of combination of ERY+DTZ (A) and DTZ+nd-DTZ (B) with HLM using Equation X (○) and Equation Y (●).

The predicted %remaining enzyme activity was calculated by Equation X and Y. The observed %remaining enzyme activity was measured from incubation of ERY and DTZ, or DTZ and nd-DTZ with HLM (1 mg) for two and five minutes. Inhibitor concentrations were at $1/2K_I$, K_I, and $2K_I$. The dotted line, solid line, and broken line represent the line of identity, regression line for data using Equation Y, and regression line data using Equation X, respectively.

Fig. 5. Percentage of remaining enzyme activity, ERY concentration, and nd-ERY concentration in incubation of ERY at various concentrations with rCYP3A4(+b5) for ten minutes (A) and percentage of remaining enzyme activity and inhibitor concentrations in incubation of ERY alone, DTZ alone, and ERY and DTZ together with rCYP3A4(+b5) for ten minutes (B). In A, ERY was incubated at 2.5 uM, 5 uM, and 10 uM. In B, ERY and DTZ were incubated at 5uM and 1 uM, respectively.

Fig. 6. Plot of predicted against observed 6β-OH TES formation rate in the incubation of TES with ERY (A) and nd-DTZ (B) with rCYP3A4(+b5) for ten minutes using Model A (○), Model B (+), and Model C (●). Concentrations used for the incubations were 10 μM, 20 μM, and 40 μM for TES, 2.5 μM, 5 μM, and 10 μM for ERY, and 0.25 μM, 0.5 μM, 2μM, and 6 μM for nd-DTZ. The dotted line, dashed line, dashed-

dotted line, and solid line represent the line of identity, regression line for data using Model A, B, and C, respectively.

Fig. 7. Plot of predicted against observed 6β-OH TES formation rate in the incubation of TES with ERY+DTZ (A) and ERY+DTZ+nd-ERY+nd-DTZ (B) with HLM for ten minutes using Model A (○), Model B (+), and Model C (●). Concentrations used for the incubations were 40 μM for TES, 5 μM, 15 μM, and 75 μM for ERY, 5 μM, 10 μM, and 40 μM for DTZ, 15 μM, 75 μM for nd-ERY, and 0.5 μM and 1 μM for nd-DTZ. The dotted line, dashed line, dashed-dotted line, and solid line represent the line of identity, regression line for data using Model A, B, and C, respectively.

Table 1. Inactivation parameters estimated for ERY, nd-ERY, DTZ, and nd-DTZ with CYP3A4+b5 and HLM.

	rCYP3A4+b5		HLM	
	3 minutes	10 minutes	3 minutes	10 minutes
ERY	55 ± 13	14.3 ± 4	73 ± 18	29 ± 19.8
nd-ERY	67 ± 11	8.2 ± 2.3	77 ± 12	19.8 ± 12.2
DTZ	5.9 ± 2.1	2.8 ± 0.5	41 ± 9	5.1 ± 3.1
nd-DTZ	0.6 ± 0.09	0.09 ± 0.2	0.8 ± 0.1	0.6 ± 0.24

Data are presented as mean ± SD.

DMD Fast Forward. Published on October 14, 2008 as DOI: 10.1124/dmd.108.022178
This article has not been copyedited and formatted. The final version may differ from this version.

Table 2. The competitive inhibition constant, K_i (μM), estimated from three-minute and ten-minute incubation in rCYP3A+b5 and HLM using competitive inhibition model.

	rCYP3A4+b5			HLM		
	K_I (μM)	k_{inact} (min^{-1})	k_{inact}/K_I ($min^{-1}\,nM^{-1}$)	K_I (μM)	k_{inact} (min^{-1})	k_{inact}/K_I ($min^{-1}\,nM^{-1}$)
ERY	5 ± 2.3	0.34 ± 0.07	70	15.7 ± 1.9	0.09 ± 0.01	6
nd-ERY	5.7 ± 1.3	0.34 ± 0.13	60	11.6 ± 1.9	0.10 ± 0.15	9
DTZ	1.3 ± 0.1	0.28 ± 0.01	220	3.7 ± 1.7	0.07 ± 0.01	20
nd-DTZ	0.3 ± 0.1	0.4± 0.03	1333	0.6 ± 0.1	0.08 ± 0.02	133

Data are presented as mean ± SD.

Table 3. The %ME and %MAE estimated for Equation X and Y for the prediction of the extent of CYP3A inhibition in the presence of multiple inhibitors in rCYP3A4+b5 and HLM.

	%ME			%MAE		
	Equation X	Equation Y	*p* value	Equation X	Equation Y	*p* value
rCYP3A4+b5						
ERY + DTZ	-0.03 ± 0.06	0.01 ± 0.06	<0.001	0.05 ± 0.04	0.04 ± 0.04	0.4
ERY + nd-ERY	-0.04 ± 0.04	-0.01 ± 0.05	<0.001	0.05 ± 0.03	0.03 ± 0.22	0.22
DTZ + nd-DTZ	-0.10 ± 0.10	-0.06 ± 0.08	<0.001	0.15 ± 0.10	0.09 ± 0.06	<0.05
All 4 compounds	0.03 ± 0.05	0.01 ± 0.07	<0.001	0.11± 0.09	0.08 ± 0.12	0.12
HLM						
ERY + DTZ	-0.03 ± 0.06	0.01 ± 0.05	<0.01	0.05 ± 0.05	0.04 ± 0.03	0.25
ERY + nd-ERY	-0.10 ± 0.07	-0.03 ± 0.06	<0.01	0.10 ± 0.07	0.05 ± 0.04	<0.05
DTZ + nd-DTZ	-0.08 ± 0.08	-0.02 ± 0.06	<0.01	0.09 ± 0.07	0.03 ± 0.03	0.02
All 4 compounds	-0.11 ± 0.09	0.04 ± 0.05	<0.01	0.11 ± 0.05	0.06 ± 0.05	0.88

Data are presented as mean ± SD.

Table 4. The % ME and %MAE estimated for Model A, B, and C for the prediction of the extent of CYP3A inhibition in the presence of TES and multiple inhibitors together in rCYP3A+b5 and HLM

	%ME					%MAE				
	Model A	*p* value*	Model B	*p* value†	Model C	Model A	*p* value*	Model B	*p* value†	Model C
rCYP3A4+b5										
ERY	0.93 ± 0.5	< 0.001	0.06 ± 0.2	0.4	-0.01 ± 0.2	0.93 ± 0.5	< 0.01	0.15 ± 0.1	0.9	0.15 ± 0.1
DTZ	0.72 ± 0.3	< 0.0001	0.20 ± 0.2	< 0.01	0.13 ± 0.2	0.72 ± 0.3	< 0.05	0.22 ± 0.2	0.2	0.16 ± 0.1
nd-ERY	1.34 ± 0.7	< 0.01	0.22 ± 0.2	0.4	0.16 ± 0.1	1.34 ± 0.6	< 0.001	0.20 ± 0.2	0.3	0.18 ± 0.1
nd-DTZ	1.00 ± 0.4	< 0.0001	0.26 ± 0.2	< 0.01	-0.07 ± 0.2	1.04 ± 0.34	< 0.0001	0.27± 0.2	0.1	0.16 ± 0.1
ERY + DTZ	0.99 ± 0.3	< 0.001	0.15 ± 0.1	< 0.01	-0.05 ± 0.2	0.99 ± 0.23	< 0.001	0.17 ± 0.2	0.2	0.06 ± 0.1
ERY + nd-ERY	1.02 ± 1.2	< 0.001	0.13 ± 0.1	< 0.01	-0.15 ± 0.1	1.00 ± 0.22	< 0.001	0.14 ± 0.1	0.1	0.09 ± 0.1
DTZ + nd-DTZ	0.90 ± 0.3	< 0.001	0.30 ± 0.3	< 0.01	-0.08 ± 0.2	0.90 ± 0.4	< 0.001	0.30 ± 0.2	0.1	0.11 ± 0.2
All 4	0.80± 0.4	< 0.001	0.32 ± 0.3	< 0.01	-0.07 ± 0.2	0.80 ± 0.4	< 0.001	0.33 ± 0.2	< 0.05	0.14 ± 0.1
HLM										
ERY	0.53 ± 0.2	< 0.05	0.22 ± 0.2	0.1	0.05 ± 0.2	0.33 ± 0.2	< 0.05	0.25 ± 0.1	0.2	0.13 ± 0.1
DTZ	0.18 ± 0.7	< 0.0001	0.41 ± 0.3	<0.01	0.01 ± 0.0	0.21 ± 0.1	0.03	0.41 ± 0.3	0.1	0.11 ± 0.1
nd-ERY	0.50 ± 0.3	< 0.0001	0.21 ± 0.2	0.01	0.07 ± 0.2	0.49 ± 0.3	< 0.01	0.22 ± 0.2	0.2	0.12 ± 0.1
nd-DTZ	0.53 ± 0.3	< 0.0001	0.83 ± 0.7	< 0.01	0.14 ± 0.2	0.53 ± 0.3	< 0.001	0.83 ± 0.7	< 0.05	0.16 ± 0.2
ERY + DTZ	0.37 ± 0.1	< 0.0001	0.17 ± 0.2	< 0.01	-0.06 ± 0.1	0.37 ± 0.1	< 0.01	0.20 ± 0.1	0.1	0.10 ± 0.0
ERY + nd-ERY	1.00 ± 0.2	< 0.0001	0.13 ± 0.1	<0.05	-0.05 ± 0.1	1.00 ± 0.2	< 0.001	0.14 ± 0.1	0.2	0.09 ± 0.1
DTZ + nd-DTZ	0.90 ± 0.4	< 0.0001	0.30 ± 0.3	< 0.001	0.08 ± 0.2	0.90 ± 0.4	< 0.01	0.29 ± 0.2	0.1	0.11 ± 0.2
All 4	1.10 ± 0.2	< 0.0001	0.90 ± 0.3	< 0.001	-0.10 ± 0.1	1.10 ± 0.2	< 0.01	0.92 ± 0.3	< 0.05	0.13 ± 0.1

Data are presented as mean ± SD.

* *p* value for the comparison of Model A and Model C

† *p* values for the comparison of Model B and Model C

Fig. 1

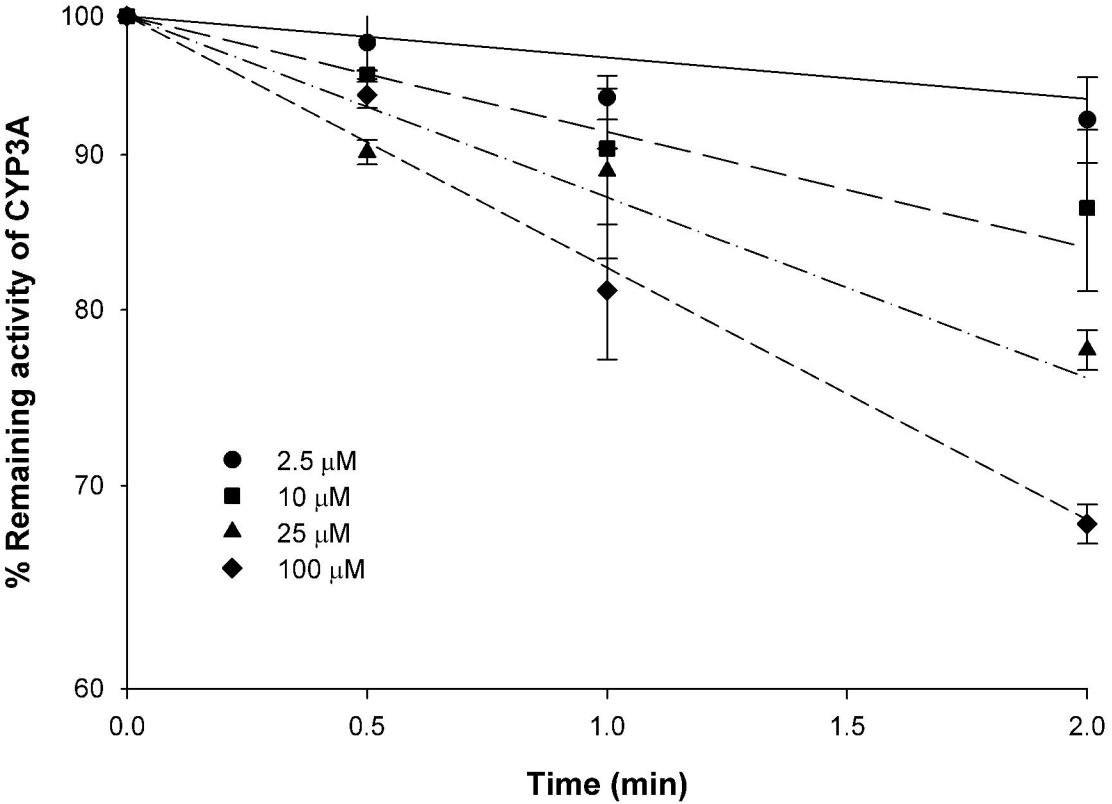
100
90
80
70
60
% Remaining activity of CYP3A
2.5 μM
10 μM
25 μM
100 μM
0.0
0.5
1.0
1.5
2.0
Time (min)

Fig. 2

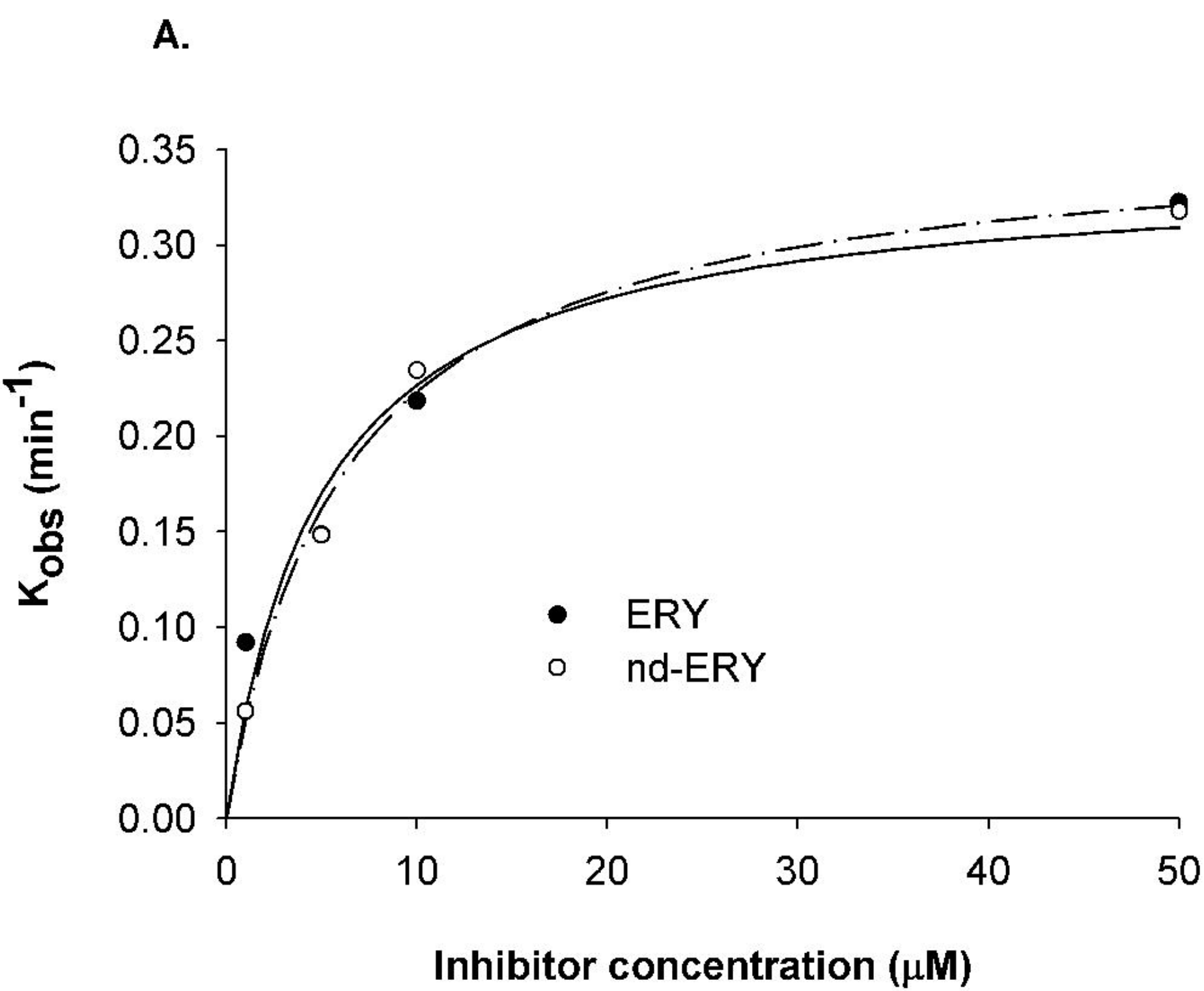
A.
0.35
0.30
0.25
0.20
0.15
0.10
0.05
0.00
K_{obs} (min^{-1})
ERY
nd-ERY
0
10
20
30
40
50
Inhibitor concentration (μM)

Fig. 2

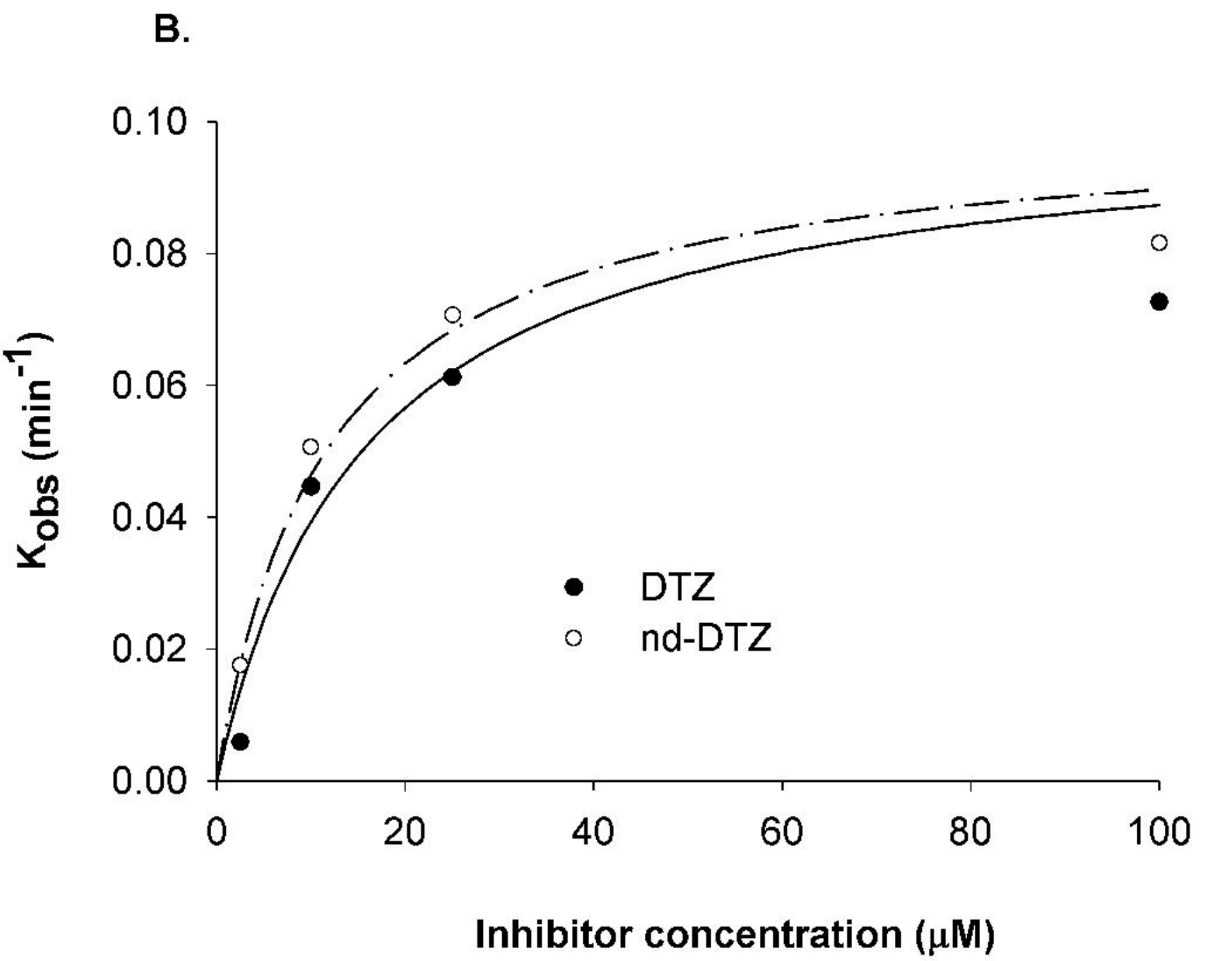
B.
0.10
0.08
0.06
0.04
0.02
0.00
K_{obs} (min^{-1})
DTZ
nd-DTZ
0
20
40
60
80
100
Inhibitor concentration (μM)

Fig. 2

c.

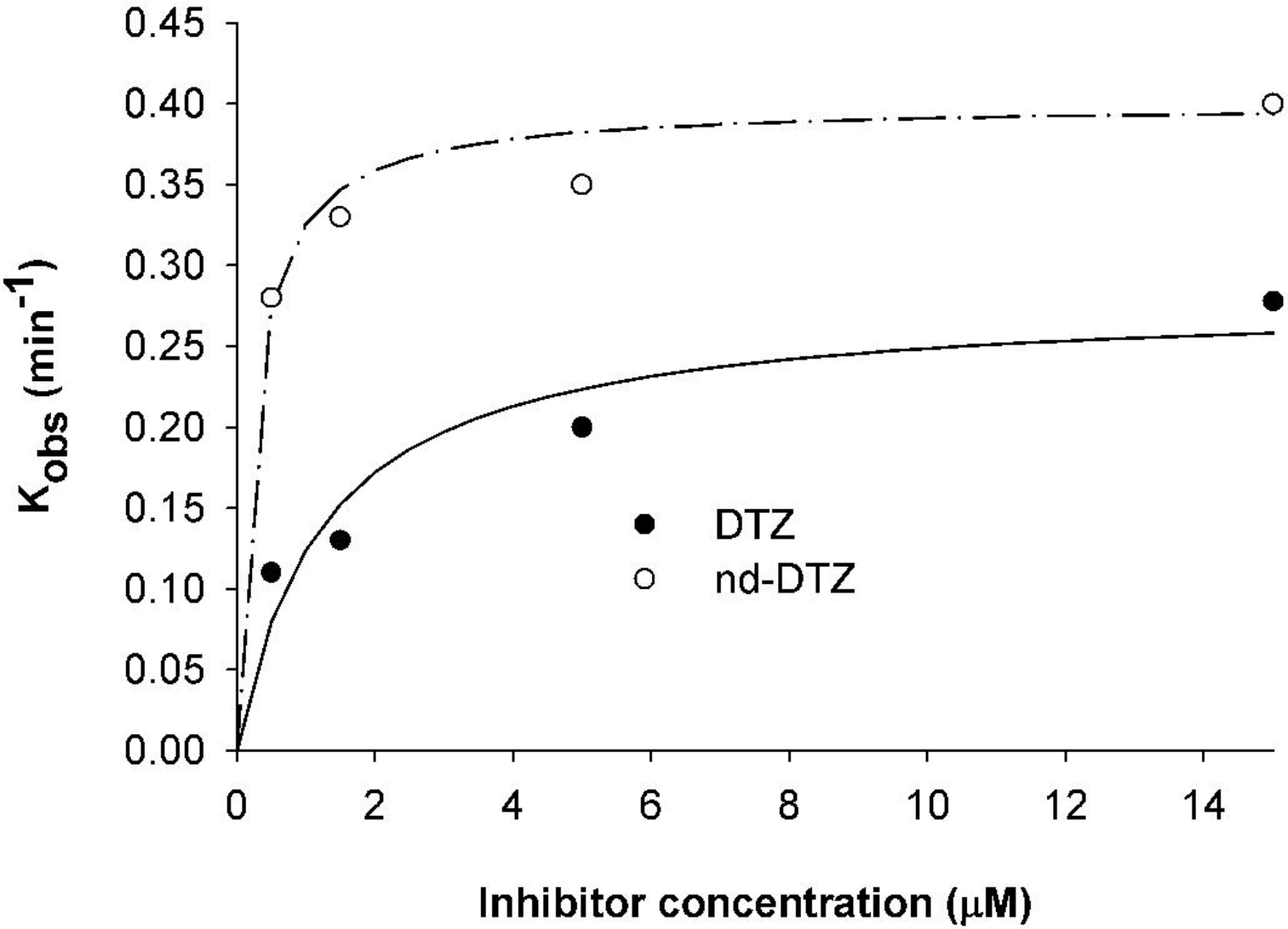
0.45
0.40
0.35
0.30
0.25
0.20
0.15
0.10
0.05
0.00
K_{obs} (min^{-1})
DTZ
nd-DTZ
0
2
4
6
8
10
12
14
Inhibitor concentration (μM)

Fig. 2

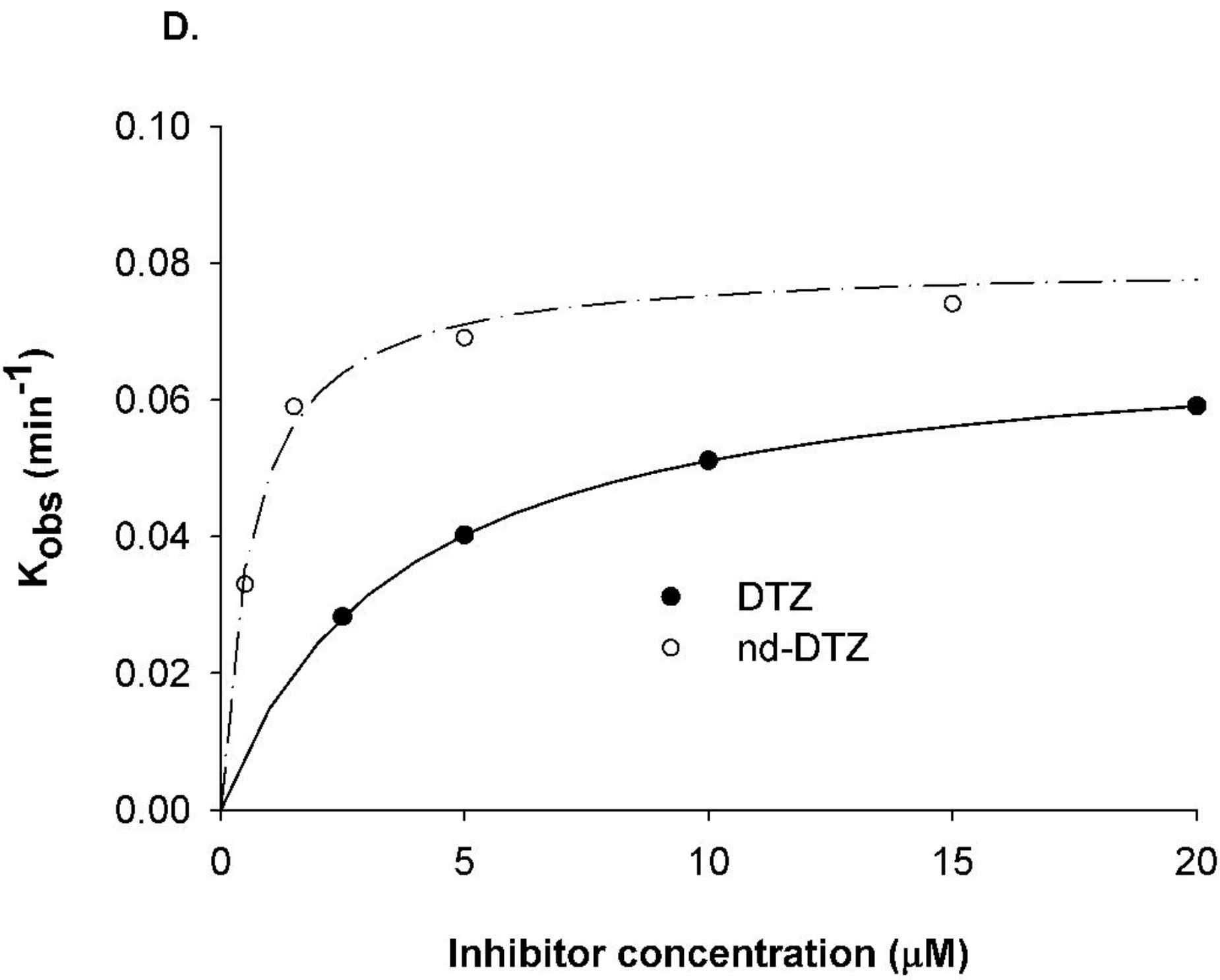
D.
0.10
0.08
0.06
0.04
0.02
0.00
K_{obs} (min^{-1})
DTZ
nd-DTZ
0
5
10
15
20
Inhibitor concentration (μM)

Fig. 3

A

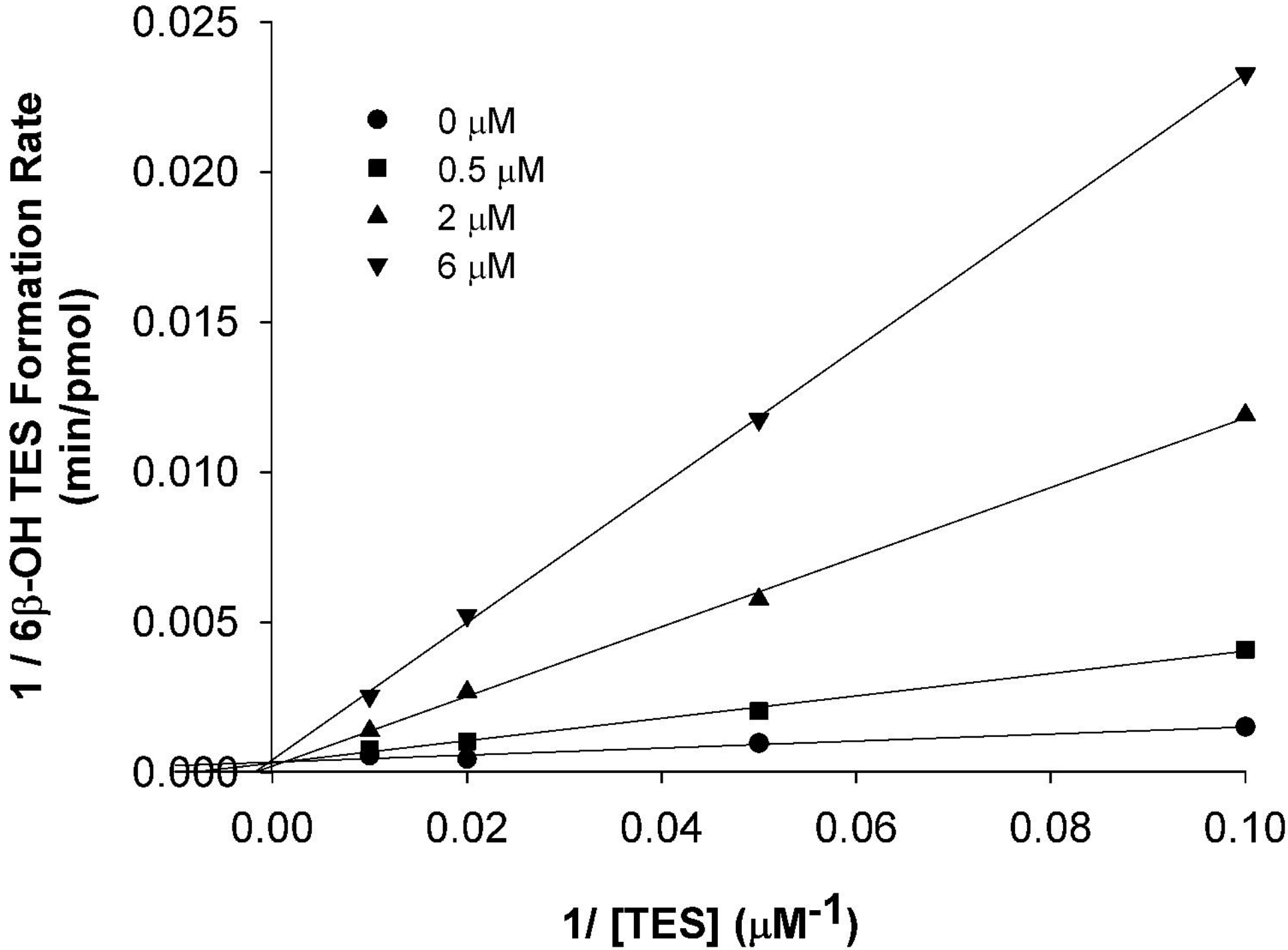
0.025
0.020
0.015
0.010
0.005
0.000
0 μM
0.5 μM
2 μM
6 μM
1 / 6β-OH TES Formation Rate (min/pmol)
0.00
0.02
0.04
0.06
0.08
0.10
1/ [TES] (μM-1)

Fig. 3

B

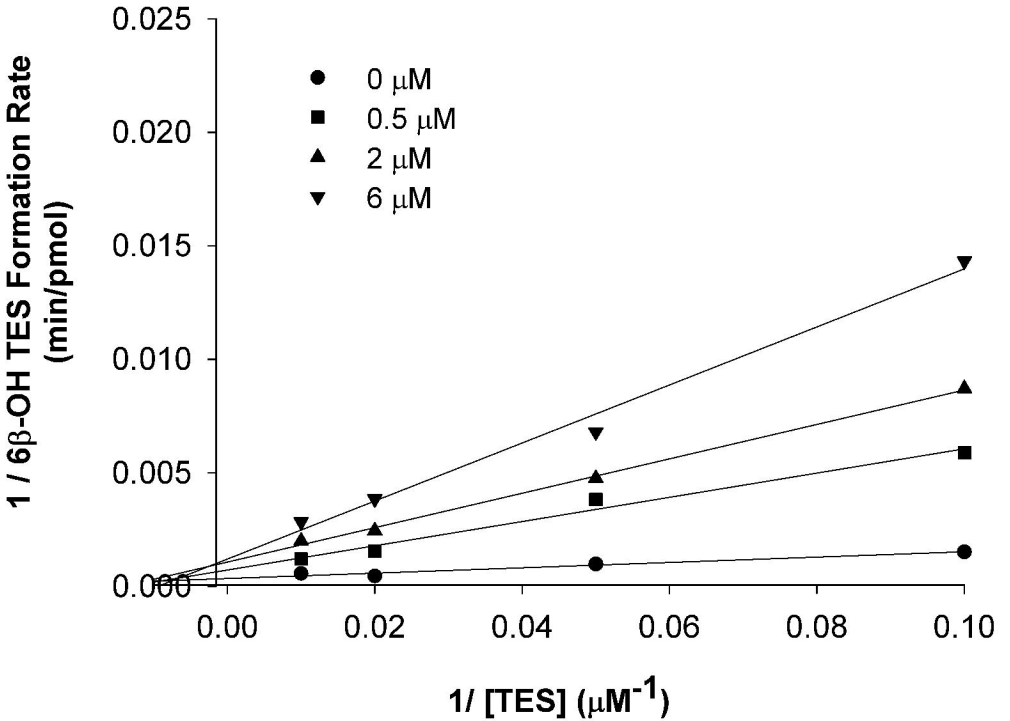
0.025
0.020
0.015
0.010
0.005
0.000
0 μM
0.5 μM
2 μM
6 μM
1 / 6β-OH TES Formation Rate (min/pmol)
0.00
0.02
0.04
0.06
0.08
0.10
1/ [TES] (μM-1)

Fig 4 A

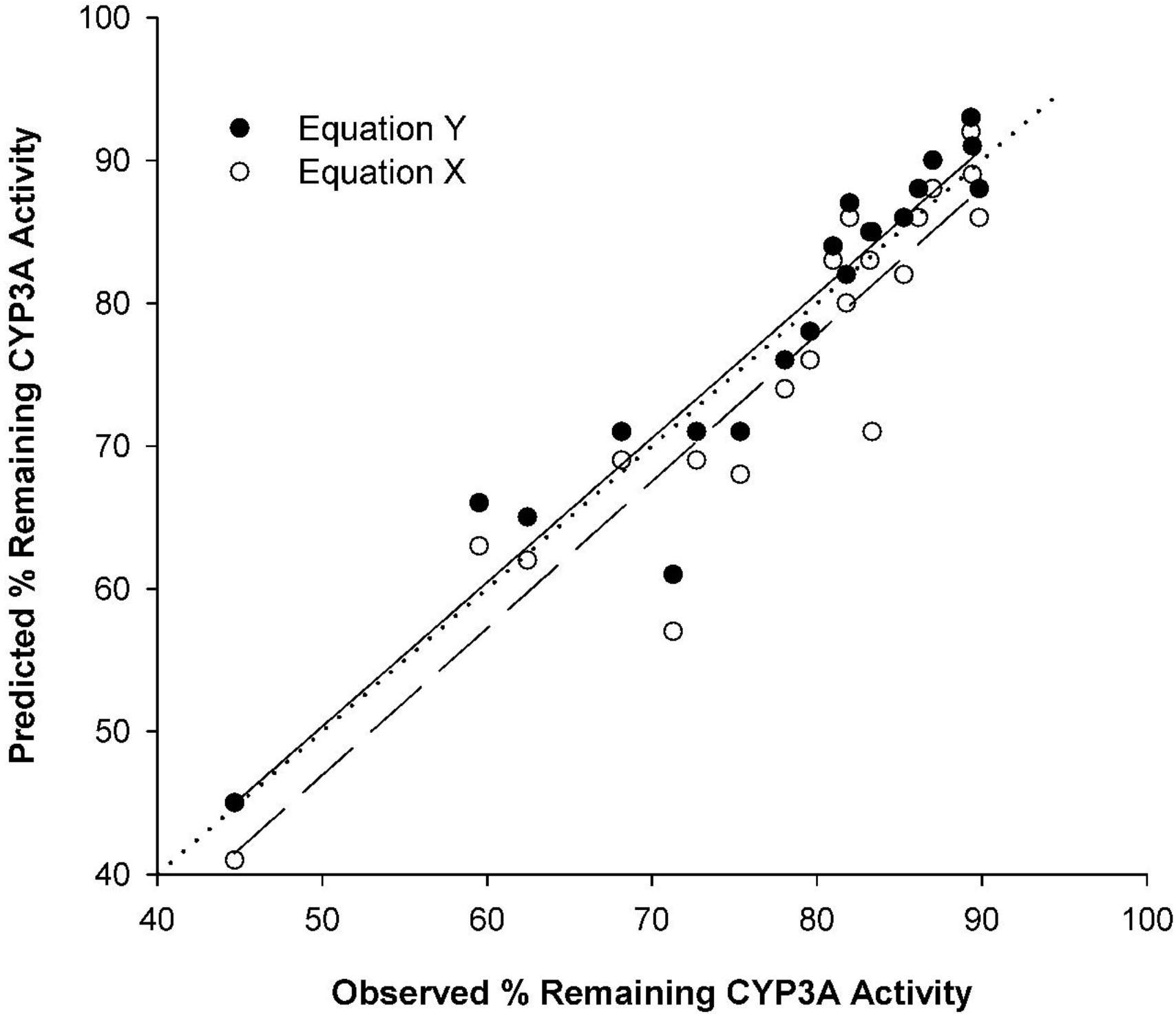
Equation Y
Equation X
Predicted % Remaining CYP3A Activity
Observed % Remaining CYP3A Activity
100
90
80
70
60
50
40
40
50
60
70
80
90
100

Fig 4. B

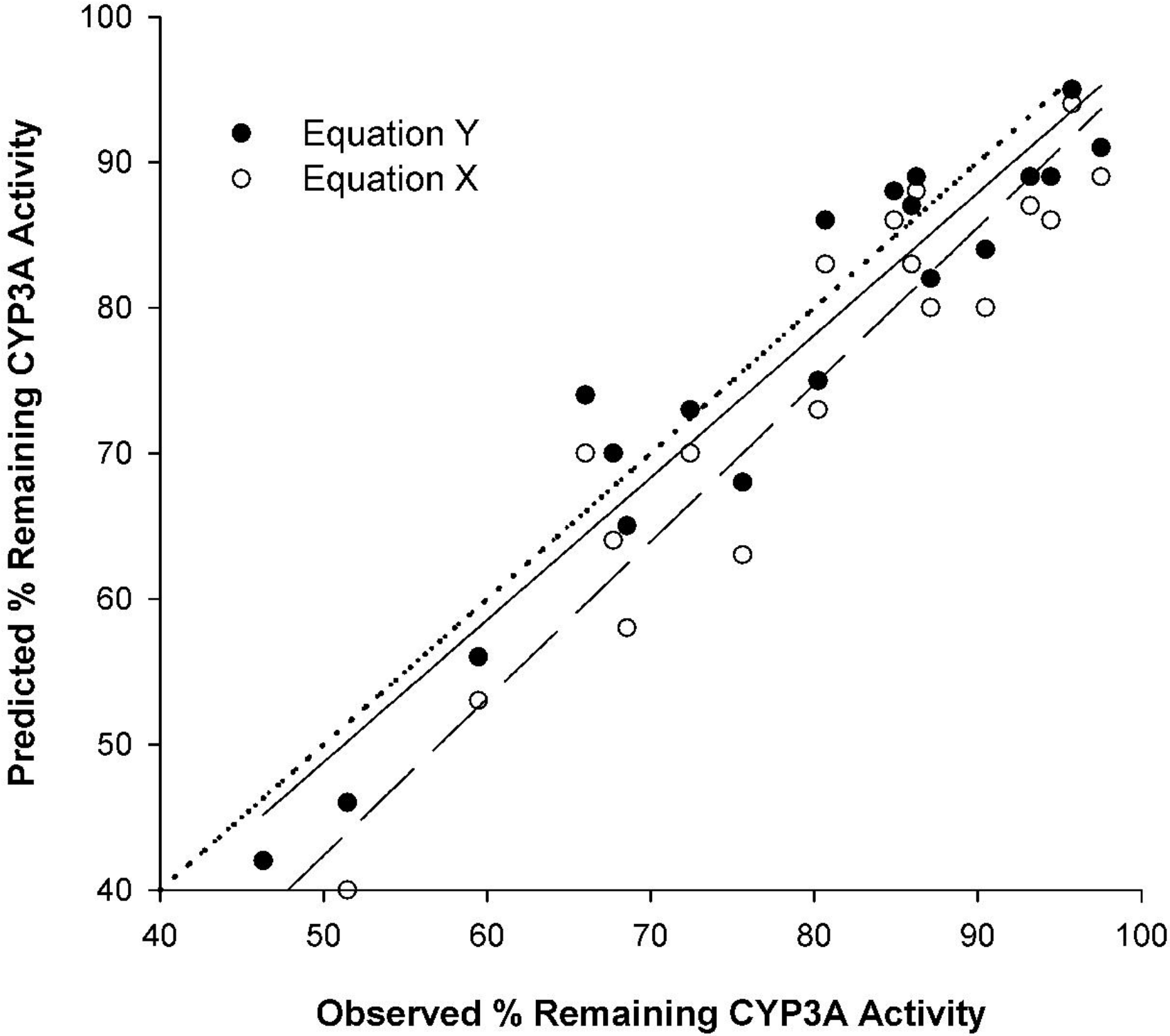
Equation Y
Equation X
Predicted % Remaining CYP3A Activity
Observed % Remaining CYP3A Activity
100
90
80
70
60
50
40
40
50
60
70
80
90
100

Fig. 5

A.

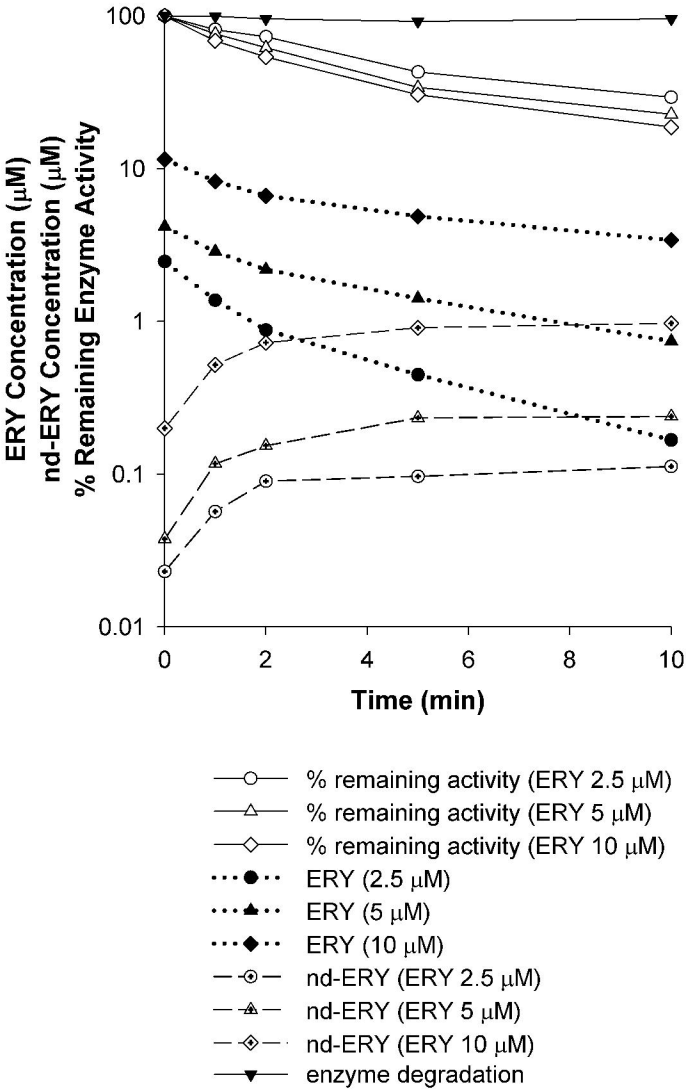
ERY Concentration (μM)
nd-ERY Concentration (μM)
% Remaining Enzyme Activity
100
10
1
0.1
0.01
0
2
4
6
8
10
Time (min)
% remaining activity (ERY 2.5 μM)
% remaining activity (ERY 5 μM)
% remaining activity (ERY 10 μM)
ERY (2.5 μM)
ERY (5 μM)
ERY (10 μM)
nd-ERY (ERY 2.5 μM)
nd-ERY (ERY 5 μM)
nd-ERY (ERY 10 μM)
enzyme degradation

Fig. 5

B.

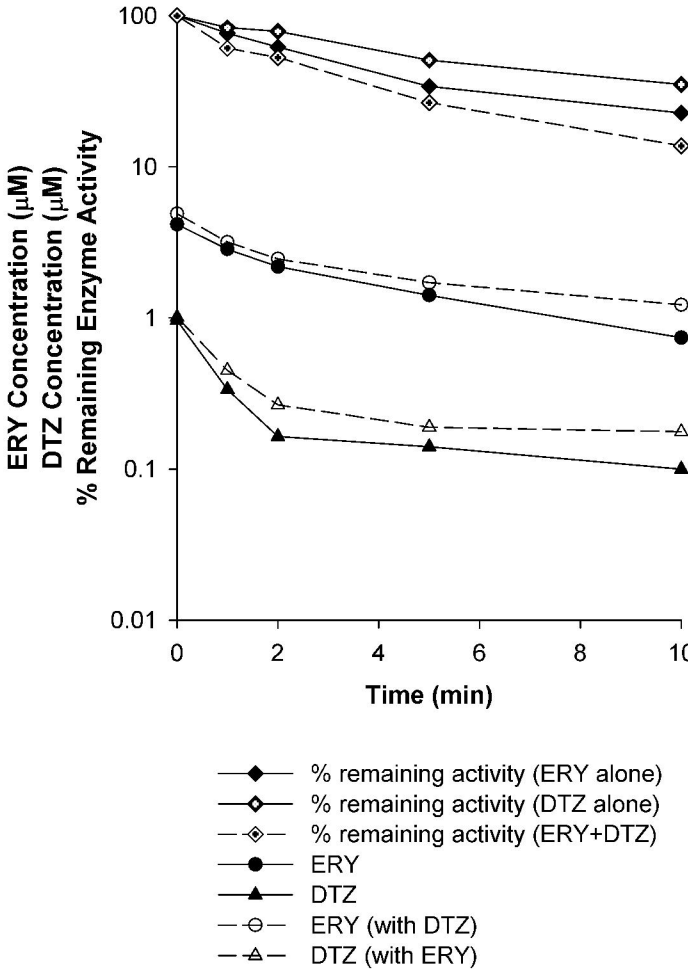
ERY Concentration (μM)
DTZ Concentration (μM)
% Remaining Enzyme Activity
100
10
1
0.1
0.01
0
2
4
6
8
10
Time (min)
% remaining activity (ERY alone)
% remaining activity (DTZ alone)
% remaining activity (ERY+DTZ)
ERY
DTZ
ERY (with DTZ)
DTZ (with ERY)

Fig. 6

A

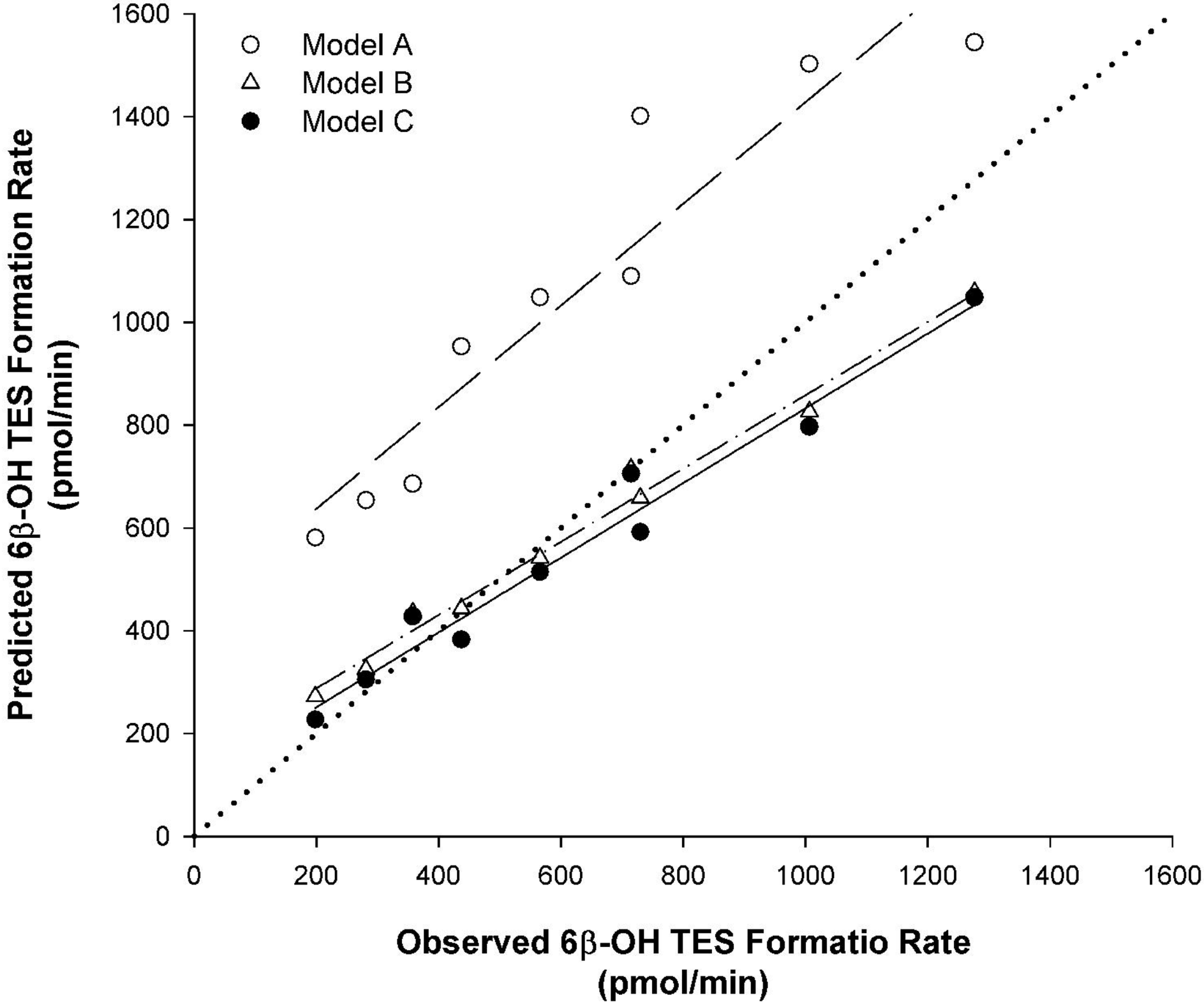
Model A
Model B
Model C
Predicted 6β-OH TES Formation Rate (pmol/min)
Observed 6β-OH TES Formatio Rate (pmol/min)
0
200
400
600
800
1000
1200
1400
1600

Fig. 6

B

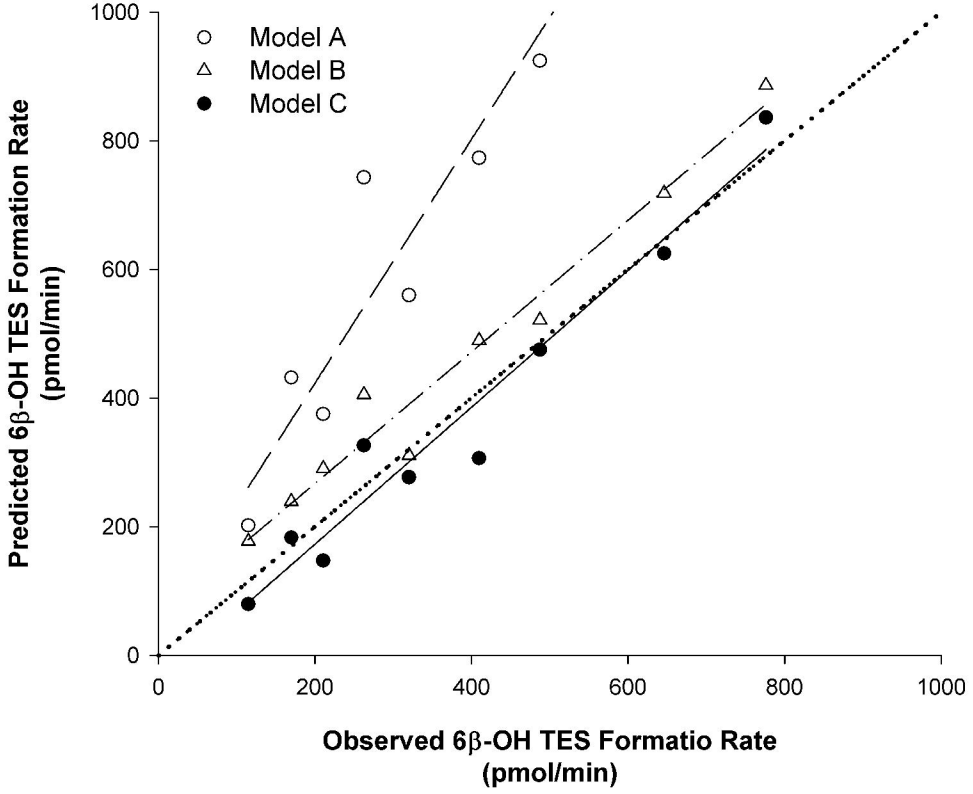
Model A
Model B
Model C
Predicted 6β-OH TES Formation Rate (pmol/min)
Observed 6β-OH TES Formatio Rate (pmol/min)
0
200
400
600
800
1000

Fig. 7

A

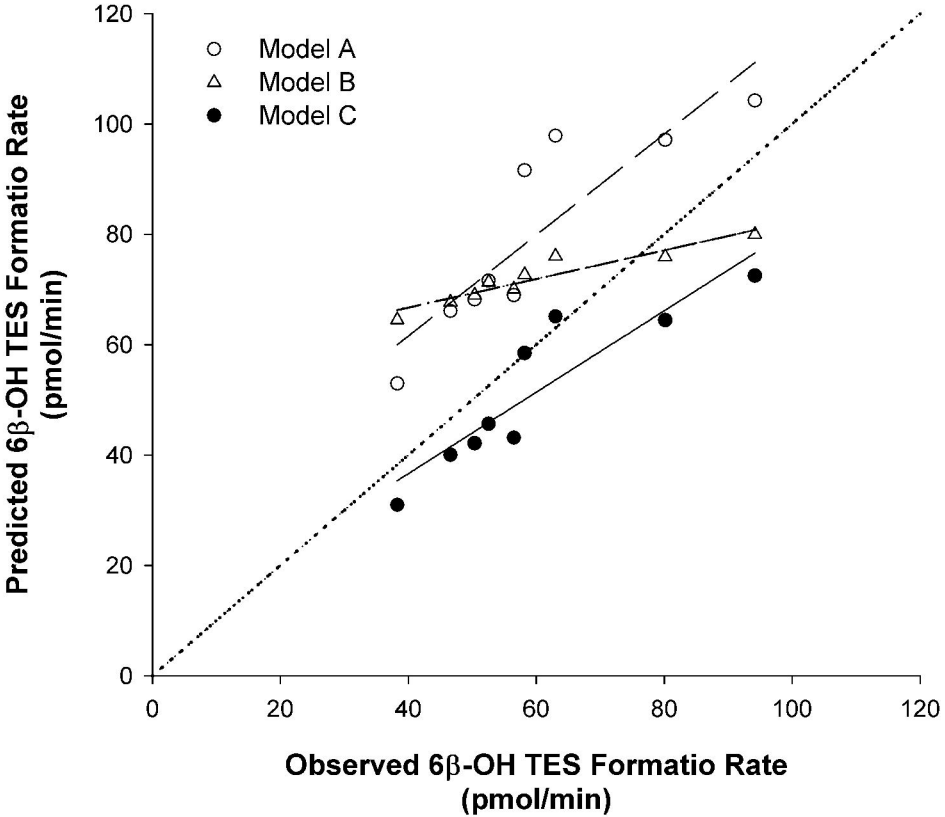
Model A
Model B
Model C
Predicted 6β-OH TES Formatio Rate (pmol/min)
Observed 6β-OH TES Formatio Rate (pmol/min)
0
20
40
60
80
100
120

Fig. 7

B

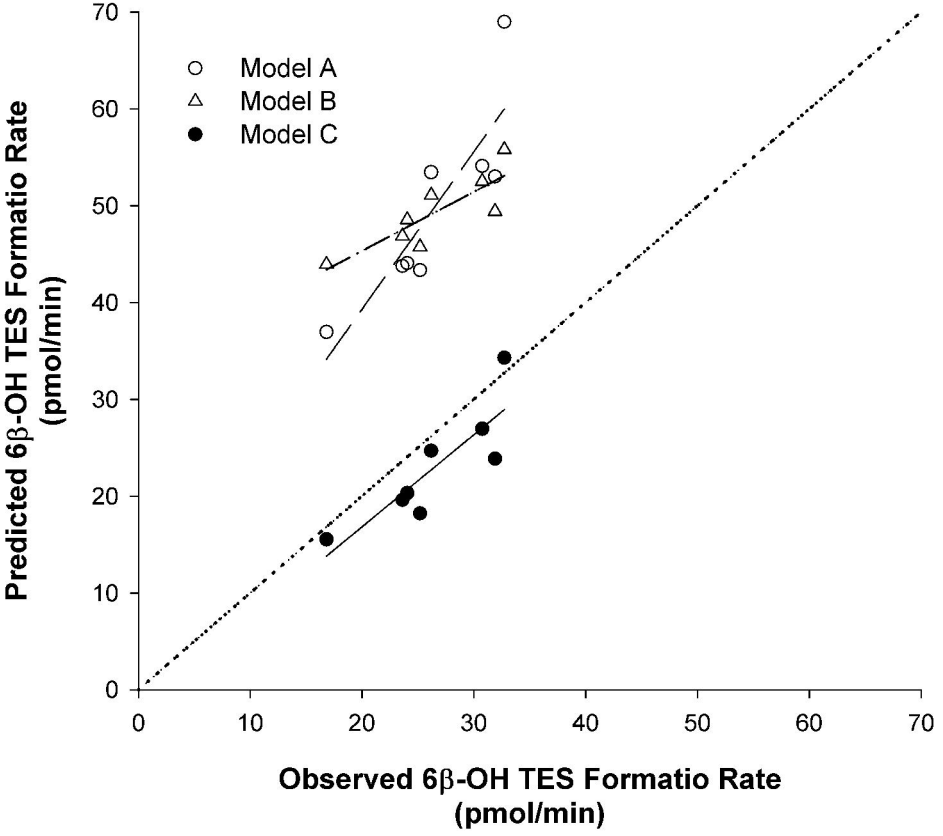
Model A
Model B
Model C
Predicted 6β-OH TES Formatio Rate (pmol/min)
Observed 6β-OH TES Formatio Rate (pmol/min)
0
10
20
30
40
50
60
70